Biointerface Research in Applied Chemistry
Open-Access Journal (ISSN: 2069-5837)

Article
Volume 16, Issue 3, 2026, 84
https://doi.org/10.33263/BRIAC163.084

Mechanistic Insights into Usnic Acid Derivatives for Gut Inflammation in Colon Cancer: An In-Silico and Systems Biology Study

Roney Miah [1,2,*], Abdul Rashid Issahaku [3], S. M. Istiaque Hamim [1], Anke Wilhelm [3], Mohd Fadhlizil Fasihi Mohd Aluwi [1,2,*]

[1] Faculty of Industrial Sciences and Technology, Universiti Malaysia Pahang, Al-Sultan Abdullah, Lebuhraya Persiaran Tun Khalil Yaakob, Gambang 26300, Kuantan, Pahang, Malaysia
[2] Centre for Bio-aromatic Research, Universiti Malaysia Pahang Al-Sultan Abdullah, Lebuhraya Persiaran Tun Khalil Yaakob, Gambang 26300, Kuantan, Pahang, Malaysia
[3] Department of Chemistry, University of the Free State, 205 Nelson Mandela Avenue, Bloemfontein 9301, South Africa
* Correspondence: psk22001@adab.umpsa.edu.my (R.M.); fasihi@umpsa.edu.my (M.F.F.M.A.);
Received: 22.01.2026; Accepted: 18.05.2026; Published: 15.06.2026

Abstract: Colon cancer (CC) is a major global health concern, accounting for approximately 930,000 deaths in 2020. Chronic intestinal inflammation contributes to CC development by promoting genetic instability, dysregulated signaling, and malignant transformation of colonic epithelial cells. In this study, we explored natural Usnic Acid (UA) derivatives as potential modulators of inflammation-associated pathways in CC using in-silico approaches. A combination of molecular docking, molecular dynamics (MD) simulations, principal component analysis (PCA), Molecular Mechanics/Generalized Born Surface Area (MM/GBSA) calculations, and network pharmacology analyses was applied. Among the screened derivatives, Usimine A (USA) exhibited the highest predicted binding affinity (-6.20 kcal/mol) relative to the reference compound 5-Fluorouracil (-5.13 kcal/mol), forming stable interactions with key residues, including a hydrogen bond with Ser530 and a C-H bond with Ser353. MD simulations indicated stable protein-ligand interactions for USA, supported by analyses of RMSD, RMSF, radius of gyration, solvent-accessible surface area, PCA, and dynamic cross-correlation. MM/GBSA analysis predicted a favorable binding free energy for USA (-59.97 ± 5.84 kcal/mol) compared to 5-Fluorouracil (-14.21 ± 1.67 kcal/mol). Network pharmacology and pathway enrichment (GO and KEGG) analyses identified multiple inflammation- and cancer-related pathways, with the HIF-1 signaling pathway (hsa04066) prominently highlighted. This pathway serves as a key regulator linking cellular hypoxia to inflammatory responses and may underlie USA's potential anti-inflammatory effects. These computational results provide mechanistic insights into UA derivatives and suggest candidates for further experimental evaluation in inflammation-associated CC.

Keywords: gut inflammation in CC; usnic acid; docking; MD simulations; mechanism study.

1. Introduction

Cancer remains a leading global health concern, with nearly 10 million deaths recorded in 2020 [1]. Among the various cancer types, colon cancer (CC) ranks as the second most common cause of cancer-related mortality [2] and the third most prevalent gastrointestinal malignancy [3], accounting for approximately 90,000 deaths each year [4]. Inflammatory

bowel diseases such as ulcerative colitis (UC) and Crohn's disease (CD) substantially increase the risk of developing CC, particularly when inflammation is chronic and widespread [5–7]. Notably, inflammation-associated CC exhibits a mortality rate exceeding 50%, which is significantly higher than hereditary or sporadic forms of the disease [2]. Persistent inflammation promotes continuous production of reactive oxygen species and pro-inflammatory cytokines, including Interleukin-6 (IL-6), Tumor Necrosis Factor-alpha (TNF-α), and Interleukin-17 (IL-17), which contribute to genomic instability, oncogenic mutations, and unregulated cell growth [6,7]. Additionally, gut microbiota imbalance (dysbiosis) aggravates CC progression by increasing intestinal permeability and sustaining inflammation [8,9]. Opportunistic pathogens such as Fusobacterium nucleatum and Bacteroides fragilis further amplify inflammation and suppress immune defenses, while cytokines like Interleukin-10 (IL-10) may paradoxically inhibit anti-tumor responses [6]. Therefore, targeting inflammation is a promising strategy for CC management, and identifying novel therapeutic targets linked to gut inflammation is essential to enhance treatment efficacy, minimize side effects, and reduce recurrence.

Cyclooxygenase 1 (COX-1) warrants renewed attention in drug discovery for gut inflammation associated with CC. Historically, it has been overshadowed by inducible COX-2, yet COX-1 maintains baseline prostaglandin production. This activity regulates mucosal homeostasis, platelet function, and the early inflammatory environment that can promote adenoma formation and tumor progression [10,11]. Unlike COX-2, which is transiently induced, COX-1 provides a continuous axis that may sustain tumor-promoting inflammatory signals from the outset. Preclinical and translational studies indicate that COX-1 expression and activity contribute to colorectal tumor cell survival and polyp development. That selective COX-1 modulation or low-dose aspirin acting via platelet COX-1 has demonstrated chemopreventive effects, highlighting its potential as an underexplored pharmacologic target [12,13]. Importantly, drug discovery must balance anti-tumor and anti-inflammatory benefits with COX-1's essential physiological roles in the gut. Strategies that are tissue-selective, platelet-targeted, or modulate downstream prostaglandin pathways may therefore enable safer and more effective interventions for inflammation-driven CC [11,14].

Natural products have historically been foundational in drug discovery, particularly for treating cancer and infectious diseases, due to their vast structural diversity and biological activity [15]. Unlike synthetic compounds, natural molecules often exhibit enhanced selectivity, multi-target engagement, and reduced toxicity, which contribute to higher success rates in clinical development [16]. Lichens, which are symbiotic associations between fungi and algae, are increasingly recognized as rich sources of pharmacologically active metabolites [17]. These metabolites exhibit diverse therapeutic properties, including anti-inflammatory [18], immunomodulatory [19], anti-diabetic [20], antiviral [21], anticancer [18], antipyretic, analgesic [22], antioxidant, and antimicrobial activities [23]. Their biosynthetic pathways, primarily the mevalonate, shikimate, and polyketide pathways, produce structurally distinct phenolics, including depsides, depsidones, quinones, and dibenzofurans [24]. Usnic acid is a dibenzofuran-type secondary metabolite derived from lichens [25,26] that exhibits various biological activities, including anti-inflammatory [27] and anti-CC [28] effects. Based on these properties, we selected natural UA derivatives, namely UA, Usimine A (USA), and Usimine B (USB), which are extracted from the Antarctic lichen Ramalina terebrata [29], for investigation in this study against the COX-1 enzyme implicated in gut inflammation in CC.

Computational methods have become essential in contemporary drug discovery, offering enhanced efficiency in identifying and optimizing therapeutic candidates. Among these, molecular docking is widely used to predict interactions between small molecules and their protein targets, providing valuable information on binding orientation and affinity, which is critical for lead compound optimization [30]. To complement this, molecular dynamics (MD) simulations deliver time-resolved insights into the structural stability and flexibility of ligand-receptor complexes, enabling a more accurate validation of docking results and a deeper understanding of molecular behavior in physiological environments [31–33]. In addition, network pharmacology contributes a system-level perspective by mapping drug-target interactions across biological networks, thereby identifying potential multi-target effects and synergistic therapeutic mechanisms [34,35]. The integration of these in-silico techniques not only reduces the time and costs associated with conventional drug development but also minimizes experimental failures and accelerates the transition from discovery to clinical research [32,36]. Together, they mark a paradigm shift toward more streamlined, cost-effective, and mechanism-driven strategies in drug development.

This study investigates the potential of natural Usnic Acid derivatives to modulate gut inflammation associated with colon cancer (CC) using an integrated in silico and mechanistic approach. We hypothesize that specific UA derivatives can form stable interactions with COX-1 and other inflammation-associated targets, thereby affecting key signaling pathways involved in CC progression. To test this hypothesis, molecular docking was performed to evaluate the binding interactions between UA derivatives and the COX-1 enzyme. The stability and reliability of these interactions were further examined using molecular dynamics (MD) simulations, complemented by principal component analysis (PCA), dynamic cross-correlation matrix (DCCM) analysis, and Molecular Mechanics/Generalized Born Surface Area (MM/GBSA) binding free energy calculations. To understand the broader molecular context, network pharmacology analysis was conducted to reveal pathways linking UA derivatives to gut inflammation in CC. Together, this integrative approach provides mechanistic insights that may inform the identification of novel therapeutic targets and the development of strategies for managing inflammation-associated CC.

2. Materials and Methods

2.1. Preparation of ligands.

The molecular structures of the natural UA derivatives, including UA, USA, and USB, were downloaded in .sdf format from the PubChem database [37].

2.2. Preparation of protein.

The crystallographic structure of the Cyclooxygenase-1 (COX-1) protein, corresponding to PDB ID: 3N8W, was obtained from the Protein Data Bank [38]. To analyze the active site and structural features of the target protein, Discovery Studio Visualizer (DSV) was employed. For molecular docking preparation, the protein structure was refined by eliminating water molecules and non-essential heteroatoms, and polar hydrogen atoms were added to ensure accurate interaction modeling [39]. The processed protein was saved in PDB format for subsequent docking simulations [40].

2.3. Molecular docking and validation.

The prepared protein structure, together with the natural UA derivatives, was subjected to molecular docking using the PyRx virtual screening tool [41,42]. Energy minimization was performed using the Universal Force Field (UFF) and the conjugate gradient method, with a maximum of 200 optimization steps [43]. The minimization process was terminated when the energy difference fell below the threshold of 0.1 kcal/mol. Following minimization, both the ligands and the protein structure were converted and saved in .pdbqt format using the Open Babel feature integrated within PyRx. The active binding site was defined in PyRx using the 'forward' option, setting the grid box coordinates to X = 15, Y = -58, and Z = 6, with dimensions adjustable manually or by the box boundaries. The docking process employed a semi-flexible approach, using the Lamarckian Genetic Algorithm for conformational search. Upon completion, AutoDock Vina generated multiple binding conformations, and the associated binding affinities were saved in .csv format. The resulting conformers were then analyzed for protein-ligand interactions using DSV. The conformer exhibiting the lowest binding energy, along with favorable non-covalent interactions, was selected as the optimal binding pose. Furthermore, docking validation was performed by re-docking the co-crystallized ligand into the same binding site.

2.4. Molecular dynamics (MD) simulations and thermodynamic calculations.

MD simulations were conducted using the GPU-accelerated Particle Mesh Ewald Molecular Dynamics (PMEMD) engine available in AMBER18 software [44,45]. The protein structure was parameterized using the AMBER ff14SB force field [46], while the ligands (natural UA derivatives) were assigned parameters from the General Amber Force Field (GAFF) [47]. The LEaP module [48] was employed to add missing hydrogen and heavy atoms to the protein. Ligand partial atomic charges were generated via the ANTECHAMBER module [49] using the Restrained Electrostatic Potential (RESP) method. To prepare the simulation system, each protein-ligand complex was solvated in a TIP3P water box, maintaining an 8.0 Å buffer from the solute surface. The systems were neutralized by adding appropriate numbers of Na^+ and Cl^- counterions. Long-range electrostatic interactions and van der Waals forces were treated using the Particle Mesh Ewald (PME) method [49]. Energy minimization was performed in two stages: the first 1000 steps utilized the steepest descent algorithm with restraints, followed by 1000 steps of conjugate gradient minimization without constraints. The systems were then gradually heated from 0 K to 310 K using a Langevin thermostat [50] with a collision frequency of 1.0 ps^{-1} and a harmonic restraint of 5 kcal/mol·$Å^2$ under the NTP ensemble. Pressure equilibration was carried out using the Berendsen barostat [51] for 5 ns while maintaining a temperature of 310 K. Hydrogen-containing bonds were constrained using the SHAKE algorithm to allow a larger integration time step. Subsequently, 200 ns of production MD simulations were executed for each system. Trajectory analyses were conducted using the CPPTRAJ and PTRAJ modules included in AMBER 18. Visualization and molecular interaction analysis were performed using UCSF Chimera and BIOVIA Discovery Studio (v19.10.18289). All simulation data and plots were generated using OriginPro version 9.1 [48].

2.5. Principal component analysis (PCA) and dynamic cross-correlation matrix (DCCM) analysis.

To assess the structural stability and flexibility of the protein-ligand complexes, RMSD and RMSF analyses were conducted using the CPPTRAJ module in AMBER18 [52]. RMSD values of the protein backbone atoms were calculated to monitor the overall stability of the system over time, while RMSF values provided insights into the residue-level flexibility throughout the simulation. Additionally, PCA was performed on the Cα atoms to explore the major conformational changes induced by ligand binding. To further examine dynamic motion correlations within the protein, DCCM analysis was performed, which quantifies the average correlated movements between Cα atom pairs over the MD trajectory. Structural mapping and visualization of the protein–ligand complexes and associated motions were performed using UCSF Chimera [53].

2.6. Binding free energy calculation.

The Molecular Mechanics/Generalized Born Surface Area (MM/GBSA) approach was employed to estimate the binding free energy (ΔG_{bind}) of the ligands with the target protein. All calculations were performed using AMBER18 with the ff14SB force field for the protein and the GAFF force field for ligands [48]. MM/GBSA analysis was carried out on snapshots extracted every 10 ns from the 200 ns MD simulation, resulting in 20 representative frames to capture the protein-ligand conformational ensemble.

The binding free energy is calculated using the following equation:

$$\Delta G_{binding} = G_{complex} - (G_{protein} + G_{ligand}) \quad (1)$$

where $G_{complex}$, $G_{protein}$, and G_{ligand} represent the free energies of the protein-ligand complex, the isolated protein, and the isolated ligand, respectively. Each free energy term is decomposed as follows:

$$G = E_{MM} + G_{solv} - TS \quad (2)$$

Where, E_{MM} = Molecular mechanics energy (sum of bonded, electrostatic, and van der Waals interactions). G_{solv} = Solvation free energy, calculated as the sum of polar (G_{GB}) and non-polar (G_{SA}) contributions. TS represents the entropic contribution to the binding free energy, which, in this study, was not explicitly calculated due to high computational cost and is therefore typically neglected in MM/GBSA estimates or approximated using normal mode analysis or quasi-harmonic methods when required.

2.7. Potential mechanism study.

The SMILES structures of natural UA derivatives were collected from the PubChem database (https://pubchem.ncbi.nlm.nih.gov/). Disease-related targets were identified using the GeneCards database (https://www.genecards.org/) by searching for the keywords “Gut Inflammation in Colon Cancer in Human” [54] and options such as “Drugs and Compounds, Disorders, Expression in Human Tissue, Function, Genomics and pathways” as well as the category “Protein Coding”. The SwissTargetPrediction (http://www.swisstargetprediction.ch/) and SuperPred (https://prediction.charite.de/index.php) databases were employed to determine

the compound-target interactions [55]. Overlapping genes were identified using Venny 2.1.0 software [56]. A compound-target network was constructed using the STRING database (https://string-db.org/cgi/input.pl) [57] and visualized with Cytoscape 3.10.2 software [58].

To investigate the association between natural UA derivatives and gut inflammation in CC at the genomic level, Gene Ontology (GO) enrichment and Kyoto Encyclopedia of Genes and Genomes (KEGG) pathway analyses were performed using the DAVID database (https://davidbioinformatics.nih.gov/summary.jsp) [59] and visualized with micro-informatics online software (https://www.bioinformatics.com.cn/). The GO analysis was categorized into three aspects: Biological Process (BP), Cellular Component (CC), and Molecular Function (MF). The top 10 results with a p-value ≤ 0.01 in each category were selected for enrichment and visualization. Additionally, a KEGG analysis of overlapping genes between the synthesized compounds and malaria was conducted to identify molecular pathways linking the compounds to gut inflammation in CC.

3. Results and Discussion

3.1. Molecular docking and validation.

Molecular docking plays a crucial role in anti-inflammatory drug discovery by predicting binding affinities and interaction modes between ligands and inflammation-related targets like COX-2 and Nuclear Factor kappa-light-chain-enhancer of activated B cells (NF-κB), aiding rational drug design [60,61]. This method enables rapid virtual screening of large compound libraries, significantly reducing time and cost compared to experimental techniques [30,60]. It also assists in identifying active sites and analyzing key interactions, which guide the optimization of drug candidates [30]. Docking enhances understanding of molecular mechanisms and selectivity, improving drug efficacy and safety [62,63]. Its integration with biological studies validates novel compounds [61,64].

To validate the docking protocol, the co-crystallized ligand was re-docked into the active site of the target protein. The resulting ligand pose closely reproduced the crystallographic conformation, with a root-mean-square deviation (RMSD) of 0.13 Å between the docked and original ligand structures (Figure 1). This low RMSD value, well below the commonly accepted threshold of 2 Å, confirms that the docking procedure is reliable and suitable for predicting ligand-protein interactions in this system.

Figure 1. Superimposition of the co-crystallized ligand (black) and the redocked ligand (yellow) in the active site of the target protein.

The present study aims to identify potential CC inhibitors targeting the COX-1 enzyme from natural UA derivatives using in silico approaches. For comparative purposes,

5-Fluorouracil was employed as the reference compound due to its established efficacy in CC therapy. 5-Fluorouracil is a well-established chemotherapeutic agent for treating CC, exerting its antitumor effects mainly by inhibiting thymidylate synthase (TS), thereby disrupting DNA synthesis, inducing apoptosis, and arresting the cell cycle via caspase activation and p53 signaling [65,66]. However, 5-Flurouracil also activates the WNT/β-catenin pathway through p53, promoting cancer stem cell (CSC) enrichment, which may contribute to tumor recurrence and resistance [67]. Beyond its anticancer role, 5-Flurouracil has complex effects on inflammation, particularly in the gastrointestinal tract. It induces oxidative stress by generating ROS, activating pro-inflammatory pathways such as NF-κB, and increasing cytokine expression (IL-1β, IL-6, TNF-α, IL-8) in intestinal and hepatic cells [68–71]. Additionally, 5-Flurouracil enhances phosphorylation of p65 and p38 in intestinal epithelial cells, contributing to mucosal injury and gut inflammation [70,71].

The molecular docking analysis provided insights into the binding affinities and interaction profiles of four compounds, namely 5-Fluorouracil (reference), UA, USA, and USB, against the target protein. UA, with a Vina score of -4.73 kcal/mol, exhibited slightly lower binding affinity compared to the reference. Nevertheless, it established notable interactions, including hydrogen bonding with Ser530 and a salt bridge with Arg120, which likely contribute to its favorable binding. It also formed C-H bonds with Ser353 and hydrophobic interactions with Ala527, Phe518, and Ile523 via alkyl and π-alkyl contacts, suggesting a stable orientation in the active pocket. USA demonstrated the strongest binding affinity among all tested compounds, with a Vina score of -6.20 kcal/mol. It engaged in a comprehensive network of interactions, such as hydrogen bonding with Ser530, a salt bridge with Arg120, and C-H bonding with Ser353. Moreover, it formed extensive hydrophobic interactions involving Leu112, Leu93, Val116, Leu357, Val349, Leu352, Ala527, Phe518, and Ile523 (Table 1 and Figure 2a). These alkyl and π-alkyl interactions contribute to its robust and stable fit within the binding site, highlighting USA as the most promising candidate in this study. USB also showed a higher binding affinity than the reference compound, with a Vina score of -5.78 kcal/mol. It formed a salt bridge with Arg120, a C-H bond with Ser353, and multiple hydrophobic interactions with Leu357, Leu352, Ala527, Phe518, and Ile523 through alkyl and π-alkyl interactions. These results indicate that USB also binds effectively within the active site and could be considered a potential inhibitor. The reference compound, 5-Fluorouracil, showed a Vina binding score of -5.13 kcal/mol. It formed key interactions with Met522 through C-H and halogen (fluorine) bonding, and amide-π stacking with Gly526. Additionally, hydrophobic π- alkyl interactions were observed with Leu352 and Ala527, indicating moderate but stable binding within the active site (Table 1 and Figure 2b).

Table 1. Molecular docking results of natural UA derivatives and reference drug 5-fluorouracil with COX-1 enzyme (PDB ID: 3N8W) for evaluating their potential as therapeutic agents against gut inflammation in CC.

Compound name	Vina Score	Bound amino acids
Reference Compound (5-Fluorouracil)	-5.13	Met522 (C-H), Met522 (Halogen: Fluorine), Gly526 (Amide-π Stacked), Leu352, Ala527 (pi-alkyl)
UA	-4.73	Ser530 (H), Arg120 (Salt Bridge/Attractive charge), Ser353 (C-H), Ala527, Phe518, Ile523 (alkyl/π-alkyl)
USA	-6.20	Ser530 (H), Arg120 (Salt Bridge/Attractive charge), Ser353 (C-H), Leu112, Leu93, Val116, Leu357, Val349, Leu352, Ala527, Phe518, Ile523 (alkyl/π-alkyl)
USB	-5.78	Arg120 (Salt Bridge/Attractive charge), Ser353 (C-H), Leu357, Leu352, Ala527, Phe518, Ile523 (alkyl/π-alkyl)

In conclusion, all tested compounds displayed significant interactions within the target protein's active site. Among them, the USA stood out due to its superior binding affinity and extensive interaction profile, suggesting its potential as a strong lead compound for further development.

In this study, the high binding affinity of USA suggests a strong and stable interaction with the COX-1 enzyme, which may translate into significant biological efficacy. COX-1 contributes to CC by sustaining basal prostaglandin synthesis that supports tumor-promoting inflammation, angiogenesis, and epithelial proliferation, particularly in early neoplastic stages [12,72]. Although COX-2 is more inducible, evidence suggests COX-1 activity in endothelial and stromal cells also facilitates colorectal tumorigenesis [73]. Compounds with higher docking affinities often demonstrate potent in vitro and in vivo inhibition of target enzymes, correlating with enhanced therapeutic outcomes [74,75]. Therefore, the strong binding of USA to the COX-1 active site indicates its potential to suppress enzyme activity, thereby mitigating inflammation-associated CC proliferation.

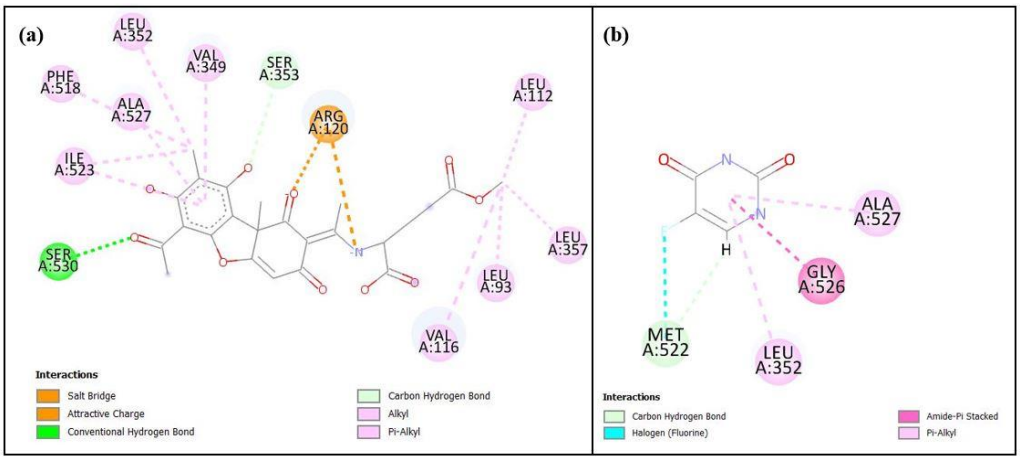

Figure 2. Molecular docking interactions of **(a)** lead compound USA; **(b)** reference drug 5-Fluorouracil with COX-1 enzyme (PDB ID: 3N8W), illustrating their binding conformations and interactions within the active site relevant to gut inflammation in CC.

Natural compounds have demonstrated strong potential for anti-inflammatory drug discovery, as evidenced by molecular docking studies that highlight their high binding affinities to key inflammatory targets. Hydro-methanolic leaf extracts with isolated compounds have shown inhibition of COX-2 and TNF-α, confirming their anti-inflammatory activity through docking results [76]. Similarly, phytoconstituents such as hederagenin, quinovic acid derivatives, and chletric acid from *Sarcocephalus pobeguinii* exhibited strong inhibition of nitric oxide production and 15-lipoxygenase (15-LOX) activity. Docking studies identified JAK2 and COX-2 as primary targets, reinforcing their potential to modulate inflammation [61]. Additionally, detailed molecular docking and dynamics studies of docosahexaenoic acid (DHA) with ALOX12 revealed key π–π stacking interactions with aromatic residues (Phe174, Phe352, His365, Phe414), contributing to substrate stability and regioselectivity [77]. Furthermore, synthetic UA derivatives significantly inhibited TNF-α and IL-1β in LPS-stimulated U937 cells, with some compounds reducing TNF-α by over 90%, outperforming prednisolone and dexamethasone. Docking confirmed stable binding to inflammatory mediators, indicating modulation of NF-κB and JAK-STAT pathways [78]. Several natural compounds, including curcumin, resveratrol, and quercetin, inhibit COX-1, reducing prostaglandin synthesis and inflammation associated with colorectal cancer [79–81].

Flavonoids such as apigenin and catechins selectively target COX-1-mediated pathways, underscoring their chemopreventive potential [82, 83]. Docking studies further reveal COX-1 selectivity of natural products: 2,3-Dihydro-3,5-dihydroxy-6-methyl-4H-pyran-4-one from *Phoenix sylvestris* exhibited strong affinity for COX-1 (-5.393 kJ/mol) over COX-2 [84], while γ-Mangostin showed a very low COX-1/COX-2 selectivity index (0.0269), indicating preferential COX-1 binding in silico [85].

3.2. MD simulations.

3.2.1. Impact of compounds binding on the conformational dynamics of the COX-1.

The therapeutic efficacy of a compound often arises from its ability to bind to a target protein and induce conformational changes that modulate the protein's activity. These molecular perturbations, caused by specific interactions between the ligand and amino acid residues, can either enhance or suppress the protein's function relative to its normal state. To investigate how the natural compounds influence the catalytic domain of the COX-1 protein, we analyzed the structural dynamics of the protein-ligand complexes. This analysis was performed over a 200 ns MD simulation, during which key parameters, including RMSD, RMSF, RoG, and SASA of individual residues, were evaluated.

3.2.2. Compounds that bind stabilize the COX-1.

RMSD plays a pivotal role in MD simulations, particularly in evaluating structural stability and the dynamic behavior of protein-ligand complexes in anti-inflammatory drug discovery. RMSD assesses atomic displacement from a reference conformation over time, offering insights into equilibration and the persistence of ligand binding [86]. A consistently low RMSD value reflects strong structural integrity and effective ligand engagement, both essential for evaluating drug efficacy and refining therapeutic candidates [87]. In the present study, the average Cα RMSD values for COX-1 were 2.00 ± 0.21 Å for the apo protein, 1.77 ± 0.31 Å for the USA complex, and 1.72 ± 0.26 Å for the 5-fluorouracil complex. These results indicate that ligand binding is associated with slightly reduced conformational deviations compared to the unbound form (Figure 3a and Table 2). Although the differences between the ligand-bound systems are modest, both complexes maintained stable trajectories throughout the simulation. The USA–COX-1 complex exhibited comparable and marginally lower fluctuations, suggesting stable accommodation within the binding site. Overall, the RMSD profiles support structural stability of the protein–ligand complexes without implying substantial differences in structural integrity. Stable binding often correlates with stronger inhibitory potency, as consistent interactions can effectively block the enzyme's catalytic activity and prevent substrate access [88]. Moreover, lower RMSD patterns are predictive of favorable pharmacodynamic behavior, indicating that the compound may retain its bioactive conformation under physiological conditions [89].

Table 2. RMSD, RMSF, RoG, and SASA values of COX-1 Enzyme in apo form (unbound) and in complex with USA and 5-fluorouracil during 200 ns MD simulations.

System	RMSD	RMSF	RoG	SASA
Apo (Unbound) Protein	2.00±0.21	0.91±0.53	24.17±0.12	23565.69±495.28
USA complex	1.77±0.31	0.90±0.49	24.14±0.09	23298.37±423.02
5-Fluorouracil complex	1.72±0.26	0.99±0.37	24.27±0.09	23745.25±419.70

RMSF is another critical descriptor in MD simulations, capturing per-residue flexibility and local motions within the protein structure. RMSF analysis is particularly useful for understanding how ligand binding modulates structural dynamics at the residue level, especially in key regions involved in anti-inflammatory activity [90]. Elevated RMSF values typically indicate flexible loops or unstable regions, whereas reduced fluctuations suggest enhanced stability upon ligand binding [86]. Here, the average RMSF for the apo protein was 0.91 ± 0.53 Å, while USA and 5-Fluorouracil complexes exhibited RMSF values of 0.90 ± 0.49 Å and 0.99 ± 0.37 Å, respectively (Figure 3b and Table 2). These findings indicate that ligand binding, particularly with USA, slightly suppressed residue-level flexibility, suggesting improved rigidity in critical regions.

RoG serves as a metric for evaluating the overall compactness of protein structures during MD simulations, reflecting changes in molecular folding and conformational stability relevant to drug binding [86,91]. A stable or reduced RoG value implies a more compact protein structure, often associated with favorable binding interactions and functional integrity [92]. RoG analysis demonstrated minimal structural variation among all systems. The apo protein showed an average RoG of 24.17 ± 0.12 Å, while the USA and 5-fluorouracil complexes exhibited values of 24.14 ± 0.09 Å and 24.27 ± 0.09 Å, respectively (Figure 3c and Table 2). The differences are small and fall within a comparable range, indicating that ligand binding did not substantially alter the protein's overall compactness. Overall, the RoG profiles suggest that all systems maintained similar structural stability throughout the simulation.

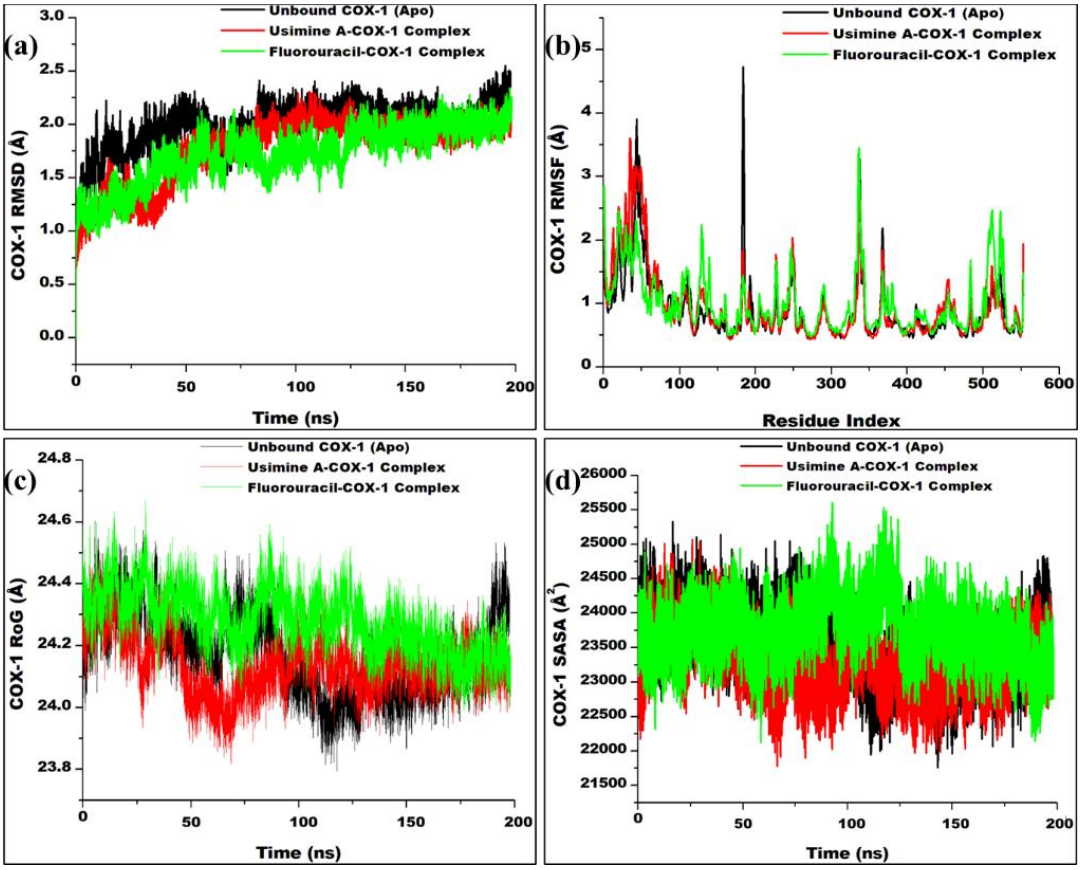

Figure 3. MD simulations profiles of the COX-1 enzyme in apo form (unbound), USA complex, and 5-Fluorouracil Complex. Plots represent **(a)** RMSD; **(b)** RMSF; **(c)** RoG; **(d)** SASA, illustrating the structural stability and dynamic behavior of each system over a 200 ns simulation time.

SASA is a fundamental parameter for characterizing the solvent exposure of protein surfaces during simulations, providing insights into conformational alterations and ligand

accessibility [93,94]. Changes in SASA indicate how binding events influence protein folding and surface interactions, which are crucial for understanding the binding efficacy of anti-inflammatory compounds [31]. In this study, the apo protein presented a SASA of $23{,}565.69 \pm 495.28$ Å², while the USA and 5-Fluorouracil complexes showed values of $23{,}298.37 \pm 423.02$ Å² and $23{,}745.25 \pm 419.70$ Å², respectively (Figure 3d and Table 2). The lower SASA of the USA complex suggests a more folded and less solvent-exposed structure, further supporting the notion of enhanced compactness and structural stability. This observation is consistent with the RMSD, RMSF, and RoG results, highlighting USA's potential to stabilize the COX-1 enzyme conformation more effectively than 5-Fluorouracil.

3.2.3. COX-1 switches react to binding site changes through correlated residual movements.

Principal Component Analysis (PCA) is an essential analytical technique in MD simulations, particularly valuable for anti-inflammatory drug discovery. By simplifying complex trajectory data into major collective motions, PCA helps identify key conformational changes and dominant dynamic patterns within protein-ligand systems. This dimensionality reduction facilitates the distinction between stable and unstable binding modes, enabling the identification of compounds with favorable interaction profiles and higher therapeutic potential [95]. By capturing large-scale structural shifts beyond the scope of traditional metrics, PCA provides critical insights into molecular flexibility, conformational stability, and energy landscapes, thereby informing rational drug design targeting inflammation-associated proteins [96].

In this study, PCA was employed to further the dynamic stability of COX-1 complexes with USA and 5-Fluorouracil. The trajectories were projected onto the first two principal components (PC1 and PC2), which represent the most significant movements observed during the simulation. As illustrated in Figure 4, the USA showed a more localized, compact clustering along the principal component axes, indicating restricted motion and enhanced conformational rigidity. In contrast, 5-Fluorouracil displayed a broader distribution, reflecting increased molecular flexibility and potentially less stable interactions throughout the simulation. These dynamic patterns support previous RMSD and SASA findings, suggesting that USA forms a more stable and consistent binding interaction with COX-1, reinforcing its promise as a potent anti-inflammatory candidate.

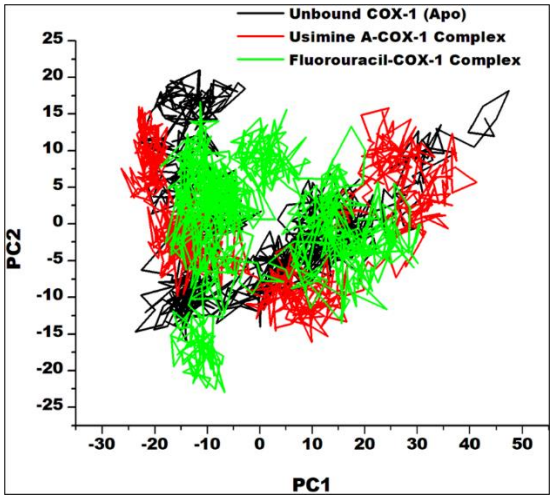

Figure 4. PCA analysis of COX-1 enzyme in apo form (unbound), USA complex, and 5-fluorouracil complex during 200 ns MD simulations. The plots depict the distribution of conformational motions along the first two principal components (PC1 and PC2), highlighting the dominant collective movements and overall conformational space sampled by each system during the simulation.

Dynamic Cross-Correlation Matrix (DCCM) analysis is a valuable approach in MD simulations, especially for elucidating the dynamic behavior of protein-ligand systems in anti-inflammatory drug discovery. By analyzing correlated atomic motions, DCCM highlights how residues move in concert or opposition, offering insights into internal flexibility, rigidity, and communication pathways within the protein structure. Such correlations are crucial for understanding how ligand binding affects protein dynamics and stability, which in turn impacts inhibitory efficacy. For instance, prior investigations into NLRP3 inflammasome inhibitors revealed that complexes with potent ligands exhibited more extensive correlated motions, particularly involving key residues such as Ala228 and Arg578, underscoring their role in modulating anti-inflammatory activity [97]. As a complementary technique to RMSD and RMSF, DCCM offers a deeper understanding of cooperative residue behavior and allosteric effects, guiding the rational design of effective anti-inflammatory agents [98].

In the current study, DCCM was employed to assess how ligand binding modulates the internal motion of the COX-1 protein. The correlation maps were generated from Cα atom fluctuations, distinguishing positively correlated movements (yellow to red) from negatively correlated ones (blue to black), as shown in Figure 5. The USA-bound complex (Figure 5a) showed more extensive and stronger positive correlations, indicating coordinated residue movements and improved structural integrity. In comparison, the 5-Fluorouracil complex (Figure 5b) and the apo form (Figure 5c) exhibited fewer such correlations, reflecting reduced dynamic coordination. These findings imply that the USA fosters a more stable and coherent conformational state, potentially contributing to its enhanced inhibitory effect. The observed dynamic differences further reinforce the superior binding and stabilization properties of USA over 5-Fluorouracil and the unliganded COX-1 structure.

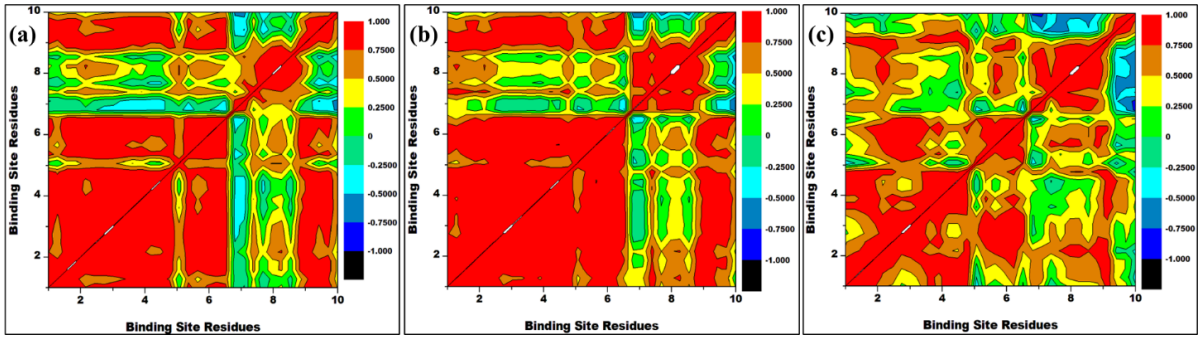

Figure 5. DCCM analysis of COX-1 Enzyme in **(a)** Apo Form (Unbound); **(b)** USA Complex; **(c)** 5-Fluorouracil Complex during 200 ns MD simulations. The matrices illustrate the correlated (positive values) and anti-correlated (negative values) atomic motions within the protein structure, revealing the effects of ligand binding on the internal dynamics and residue communication patterns.

3.2.4. Binding free energy calculations.

MM/GBSA analysis is a widely utilized method in MD simulations to estimate ligand-binding free energies with reasonable computational efficiency and high predictive value. In the context of anti-inflammatory drug discovery, MM/GBSA is a reliable approach for quantifying the strength and stability of interactions between candidate compounds and target proteins implicated in inflammatory pathways [99,100]. By integrating molecular mechanics energy components with solvation models, this method captures key thermodynamic factors governing binding affinity, providing insights critical for ranking and optimizing lead compounds. When combined with machine learning, MM/GBSA predictions become even

more powerful, enhancing the identification of high-affinity ligands for inflammation-related targets [100].

In the present investigation, MM/GBSA calculations were performed to evaluate the binding affinities of USA and 5-Fluorouracil with the COX-1 enzyme. The computed binding free energies ($\Delta G_{binding}$) were dissected into their respective energy components to understand better the driving forces behind each ligand's interaction profile. As detailed in Table 3, the USA showed a markedly more favorable binding energy of -59.97 ± 5.84 kcal/mol, in contrast to -14.21 ± 1.67 kcal/mol for 5-Fluorouracil. This substantial difference suggests that the USA engages more robustly with the COX-1 active site. The enhanced binding of USA is likely influenced by its greater molecular flexibility, which may allow it to adapt its conformation to optimize interactions with key residues. Conversely, the relatively rigid scaffold of 5-Fluorouracil may restrict its ability to form multiple stabilizing contacts. Collectively, the MM/GBSA findings reinforce the superior binding efficiency of USA, highlighting its promise as a potential COX-1 inhibitor in anti-inflammatory therapy.

Table 3. Binding free energy analysis using the MM/GBSA method of the USA and 5-fluorouracil complexes with COX-1 enzyme during 200 ns MD simulations.

	ΔE_{vdw} (kcal/mol)	ΔE_{ele} (kcal/mol)	ΔG_{gas} (kcal/mol)	ΔG_{sol} (kcal/mol)	ΔG_{bind} (kcal/mol)
USA complex	-59.51 ± 4.35	-78.57 ±12.72	-138.09±11.96	78.12 ±8.35	-59.97±5.84
5-Fluorouracil complex	-18.94 ± 1.78	-15.28 ± 2.61	-34.22 ± 2.47	20.01 ± 1.89	-14.21±1.67

3.3. Potential mechanism study.

A total of 755 gut inflammation in CC-related targets was retrieved from the GeneCards database (Table S1), of which all were unique (Table S2). Additionally, 106 USA-related targets were identified from the SwissTargetPrediction database (Table S3), and 81 targets were identified from the SuperPred (Table S4) database, with 181 being unique targets (Table S5). The intersection of the 755-gut inflammation in CC-related targets and the 181 compound-related targets revealed 19 overlapping targets (Figure 6 and Table S6).

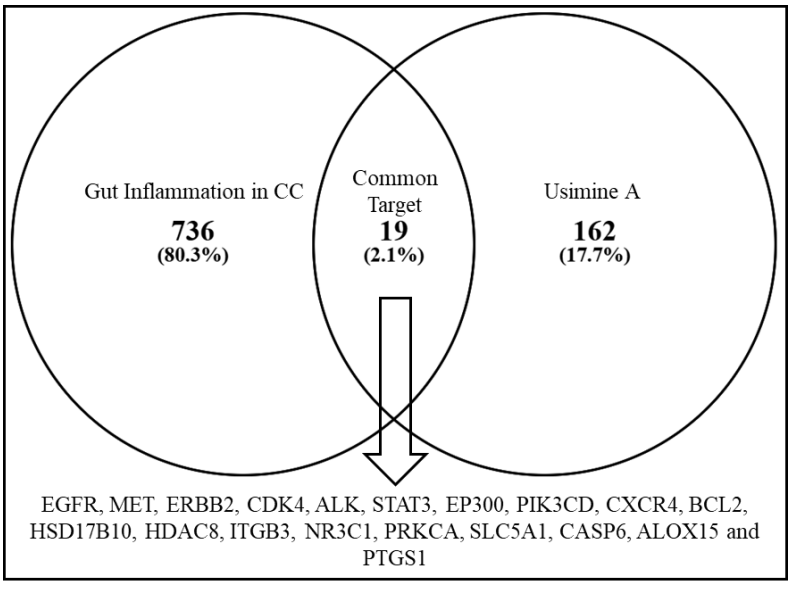

Figure 6. Venn diagram illustrating the overlap between USA-associated targets and gut inflammation in CC-related targets. The diagram highlights the shared core targets and the unique targets specific to each dataset, providing insights into the potential therapeutic relevance of USA in gut inflammation associated with CC.

To further explore the potential molecular mechanisms of USA, a protein-protein interaction (PPI) network was constructed based on the 19 overlapping target genes using the STRING database (Table S7). The PPI network was generated by excluding isolated targets and setting the interaction score threshold between connected nodes to >0.726 (Figure 7a). The network consisted of 19 connected nodes and 62 edges, with an average degree value of 6.53. The PPI network was visualized using Cytoscape 3.10.2 software (Figure 7b). Furthermore, the 31 overlapping genes were subjected to GO and KEGG analyses using the DAVID software.

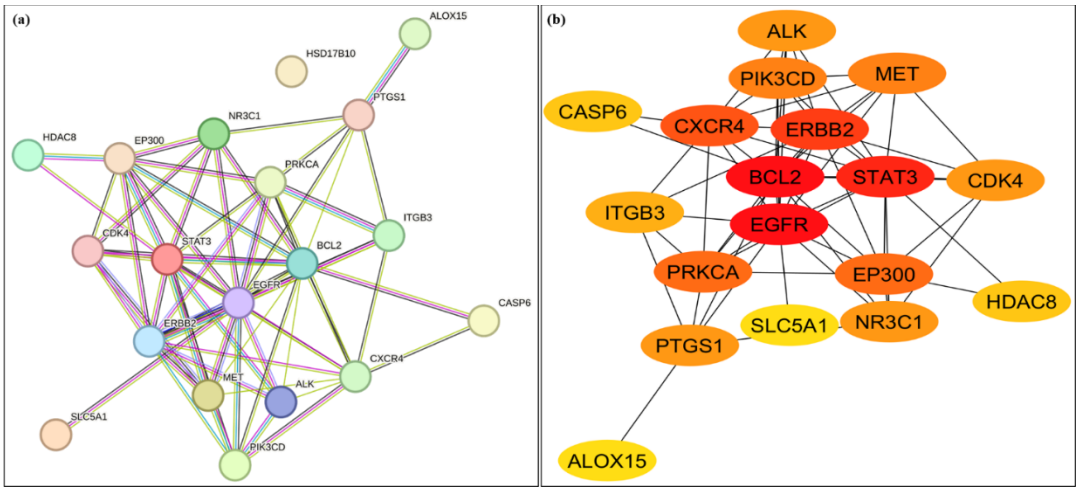

Figure 7. PPI Networks of Key Targets Associated with the USA and Gut Inflammation in CC. **(a)** PPI network constructed using STRING database, illustrating predicted functional associations among the targets; **(b)** Visualization and topological analysis of the PPI network performed using Cytoscape 3.10.2 software, highlighting hub genes and key interaction clusters relevant to the therapeutic action of USA.

To explore the biological relevance of USA, we performed GO annotation and KEGG pathway enrichment analyses on 19 overlapping genes identified from USA-gut inflammation in CC target interactions. GO analysis, conducted via the DAVID database, revealed enrichment in 78 biological processes (BP), 21 cellular components (CC), and 37 molecular functions (MF) terms (Tables S8–S10). Among the top 10 BP terms ($p \leq 0.01$) included vascular endothelial growth factor signaling pathway, regulation of cell population proliferation, vascular endothelial growth factor receptor-1 signaling pathway, platelet-derived growth factor receptor-alpha signaling pathway, macrophage colony-stimulating factor signaling pathway, Kit signaling pathway, brain-derived neurotrophic factor receptor signaling pathway, platelet-derived growth factor receptor-beta signaling pathway, hepatocyte growth factor receptor signaling pathway, and collagen-activated tyrosine kinase receptor signaling pathway (Figure 8a and Table S8). In the CC category, the top 10 targets were receptor complex, protein-containing complex, cytoplasm, nuclear membrane, basal plasma membrane, plasma membrane, alphav-beta3 integrin-PKCalpha complex, ruffle membrane, apical plasma membrane, and cytosol (Figure 8a and Table S9). Furthermore, the top 10 targets of MF analysis were boss receptor activity, platelet-derived growth factor alpha-receptor activity, brain-derived neurotrophic factor receptor activity, placental growth factor receptor activity, macrophage colony-stimulating factor receptor activity, hepatocyte growth factor receptor activity, protein tyrosine kinase collagen receptor activity, insulin receptor activity, GPI-linked ephrin receptor activity, and stem cell factor receptor activity (Figure 8a and Table S10).

KEGG enrichment analysis (Table S11) revealed that most pathways were cancer-related, suggesting that USA could inhibit gut inflammation in CC. Among 72 KEGG pathways, the top 10 pathways were non-small cell lung cancer, EGFR tyrosine kinase inhibitor

resistance, pathways in cancer, HIF-1 signaling pathway, MicroRNAs in cancer, focal adhesion, proteoglycans in cancer, human cytomegalovirus infection, pi3k-akt signaling pathway, and pancreatic cancer (Figure 8b and Table S11). Among these pathways, the HIF-1 signaling pathway plays a pivotal role in inflammation drug discovery by regulating immune cell metabolism and inflammatory responses (Figure 9). Under hypoxic conditions, HIF-1α accumulates due to inhibition of prolyl hydroxylase (PHD) and of factors that inhibit HIF (FIH), forming an active heterodimer with HIF-1β that binds hypoxia response elements to induce genes involved in angiogenesis, cell migration, and cytokine production [101]. HIF-1α modulates macrophage polarization, dendritic cell maturation, and T cell differentiation, thereby influencing inflammatory processes [102,103]. Metabolic intermediates, such as succinate, stabilize HIF-1α in activated macrophages, promoting proinflammatory gene expression, such as IL-1β, which is critical in autoimmune inflammation [103]. Targeting the PI3K/Akt/mTOR pathway to regulate HIF-1α expression offers therapeutic potential in controlling inflammation [101]. Consequently, HIF-1 signaling is a promising target for the development of novel anti-inflammatory drugs.

HIF-1 sits at the nexus of hypoxia, inflammation, and tumor biology and, therefore, is a pivotal pathway to consider when designing COX-1–targeted therapies for gut inflammation in CC. HIF-1α drives transcriptional programs that rewire metabolism, promote angiogenesis (via VEGF), and modulate immune responses in the tumor microenvironment, amplifying inflammatory circuits that can feed prostaglandin production [104]. Increased prostanoid (e.g., PGE_2) signaling, which depends on cyclooxygenase activity, can itself stabilize HIF-1α and potentiate downstream pro-tumorigenic and pro-inflammatory effects, thereby creating a bidirectional feed-forward loop linking COX activity and HIF signaling [105,106]. Although COX-1 has traditionally been viewed as a constitutive, homeostatic isoform, emerging evidence indicates COX-1 contributes to prostanoid pools in the tumor/stroma and may cooperate with HIF-driven pathways in colorectal carcinogenesis, making selective modulation of COX-1 a plausible strategy to blunt HIF-associated inflammation without the toxicity of nonselective COX inhibition [11,107]. Mechanistically, COX-1 focused drug discovery should therefore assess effects on (1) HIF-1α stabilization and transcriptional outputs (VEGF, glycolytic enzymes), (2) PGE_2 synthesis and receptor signaling, and (3) immune and epithelial barrier readouts in hypoxic versus normoxic conditions; these assays will reveal whether COX-1 inhibition breaks the HIF-prostanoid inflammatory loop or inadvertently impairs beneficial HIF-mediated mucosal defenses reported in some intestinal injury models [107,108]. Together, targeting COX-1 in the context of HIF-1 biology offers a nuanced opportunity to reduce tumor-associated gut inflammation in CC, but success will depend on careful pharmacologic selectivity and functional profiling in hypoxic, inflammation-rich tumor microenvironments [11,104].

In this study, molecular docking analysis revealed that USA exhibited a strong binding affinity toward COX-1 (-6.20 kcal/mol), surpassing the reference compound 5-Fluorouracil (-5.13 kcal/mol). The docking pose indicated multiple stabilizing interactions within the COX-1 catalytic pocket, suggesting a favorable inhibitory conformation. MD simulations further confirmed the complex's stability, as evidenced by consistent RMSD, RMSF, Rg, and SASA profiles. Additionally, binding free energy calculations supported these findings, with USA showing a superior free energy (-59.97 ± 5.84 kcal/mol) compared to the reference (-14.21 ± 1.67 kcal/mol). Collectively, these results indicate that USA may inhibit COX-1 activity,

leading to downregulation of HIF-1 signaling and potential attenuation of hypoxia-driven angiogenic and metabolic processes.

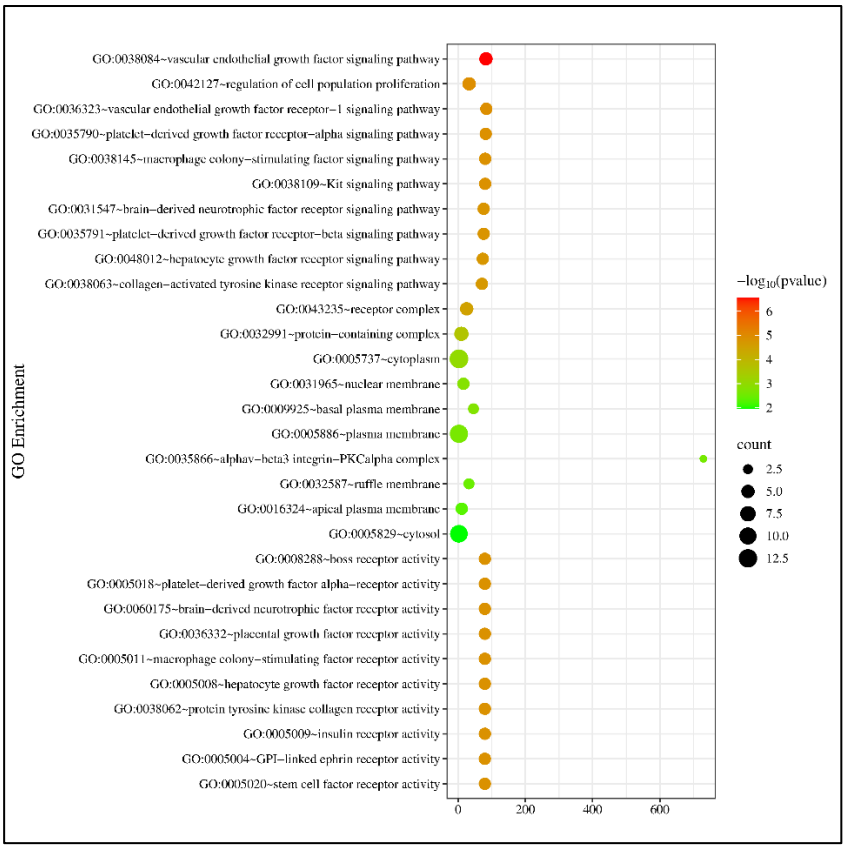

(a)

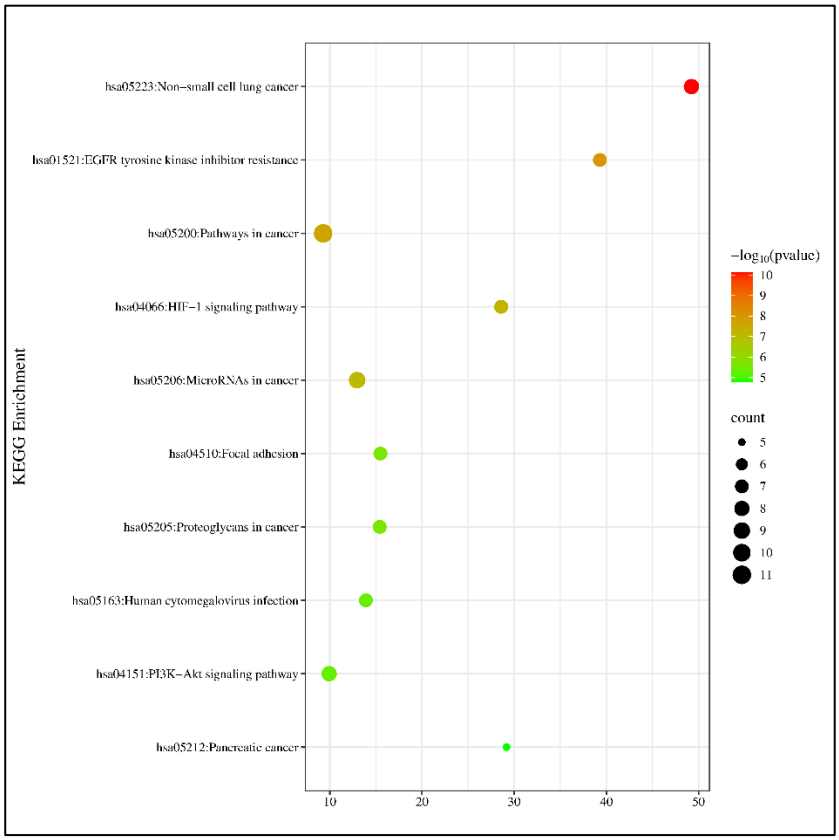

(b)

Figure 8. Functional enrichment analyses of overlapping targets between USA and gut inflammation in CC. **(a)** GO functional enrichment analysis illustrating the top biological processes, molecular functions, and cellular components associated with the shared targets; **(b)** KEGG pathway enrichment analysis highlighting the most significantly enriched signaling pathways potentially involved in the therapeutic effects of USA against gut inflammation in CC.

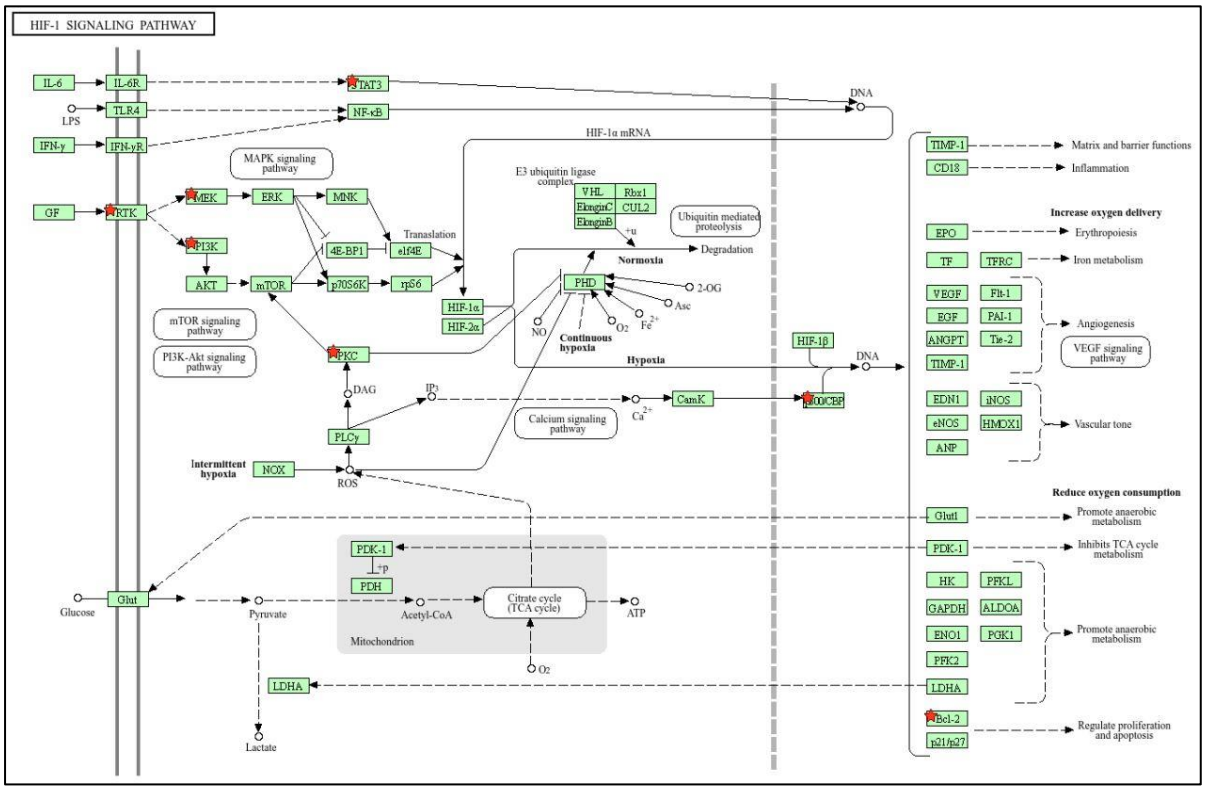

Figure 9. KEGG pathway map of hsa04066: HIF-1 signaling pathway. Red-marked nodes indicate potential therapeutic targets of USA involved in gut inflammation associated with CC, highlighting key molecular interactions and regulatory components modulated by USA within this pathway.

3.4. Limitations of the study.

The present study is entirely computational, employing in-silico approaches such as molecular docking, molecular dynamics (MD) simulations, and binding free energy analyses to explore the potential inhibitory interactions of three natural UA derivatives with COX-1 and their possible effects on the HIF-1 signaling pathway. While these methods provide valuable preliminary insights into ligand-protein interactions, binding stability, and energetic favorability, they rely on static or semi-dynamic protein models and cannot fully capture the complexity of biological systems. Notably, the accuracy of the predictions depends on the chosen protein structure, and using an inappropriate or non-physiological COX-1 conformation could compromise the reliability of the results. Furthermore, computational models do not account for crucial factors, such as cell permeability, metabolic stability, enzymatic regulation, or off-target interactions, all of which determine a compound's actual pharmacological efficacy. Consequently, the predicted inhibitory effect of USA on COX-1 and the subsequent modulation of HIF-1 signaling must be experimentally validated. Future studies should include *in vitro* enzyme inhibition assays, cell-based HIF-1α reporter assays, and *in vivo* investigations to evaluate efficacy, bioavailability, and safety. Until such experimental evidence is obtained, the results should be considered hypothesis-generating. Additionally, because COX-1 contributes to colorectal tumorigenesis by maintaining constitutive prostaglandin E_2 (PGE_2) levels that support angiogenesis, epithelial proliferation, and chronic inflammation [72,109,110], systemic inhibition may lead to off-target effects. Therefore, experimental validation is essential to confirm the biological relevance, therapeutic potential, and safety of USA.

4. Conclusions

The comprehensive in-silico analysis conducted in this study suggests that the USA may interact with the COX-1 enzyme, exhibiting favorable binding affinity, binding free energy, and stable interaction profiles compared to the reference compound 5-fluorouracil. Molecular docking, MD simulations, MM/GBSA calculations, and network pharmacology analyses indicate potential modulation of key signaling pathways involved in CC-associated gut inflammation. These computational results are hypothesis-generating and provide a basis for further experimental investigation. To confirm enzymatic inhibition, pathway modulation, and therapeutic relevance, additional in vitro, in vivo, and clinical studies are required.

Author Contributions

Conceptualization, M.R.; formal analysis, M.R., A.R.I., and S.M.I.H.; data curation, M.R., A.R.I., and S.M.I.H.; writing—original draft preparation, M.R., A.R.I., and S.M.I.H.; writing—review and editing, A.W. and M.F.F.M.A. All authors have read and agreed to the published version of the manuscript.

Institutional Review Board Statement

Not applicable.

Informed Consent Statement

Not applicable.

Data Availability Statement

Not applicable.

Funding

No funding was obtained for this study.

Acknowledgments

Thanks to the Faculty of Industrial Sciences and Technology, Universiti Malaysia Pahang, Al-Sultan Abdullah, Lebuhraya Persiaran Tun Khalil Yaakob, Kuantan, Pahang, Malaysia.

Conflicts of Interest

The author claims that their interests are not in conflict.

Abbreviations

The following abbreviations are used in this manuscript:

Abbreviation	Definition
CC	Colon Cancer
UA	Usnic Acid
MD	Molecular Dynamics
PCA	Principal Component Analysis
MM/GBSA	Molecular Mechanics/Generalized Born Surface Area
USA	Usimine A

Abbreviation	Definition
USB	Usimine B
RMSD	Root Mean Square Deviation
RMSF	Root Mean Square Fluctuation
RoG	Radius of Gyration
SASA	Solvent-Accessible Surface Area
DCCM	Dynamic Cross-Correlation Matrix
GO	Gene Ontology
KEGG	Kyoto Encyclopedia of Genes and Genomes
UC	Ulcerative Colitis
CD	Crohn's Disease
IL-6	Interleukin-6
TNF-α	Tumor Necrosis Factor-alpha
IL-17	Interleukin-17
IL-10	Interleukin-10
COX-1	Cyclooxygenase-1
COX-2	Cyclooxygenase-2
PDB	Protein Data Bank
DSV	Discovery Studio Visualizer
UFF	Universal Force Field
PMEMD	Particle Mesh Ewald Molecular Dynamics
GAFF	General Amber Force Field
RESP	Restrained Electrostatic Potential
BP	Biological Process
CC	Cellular Component
MF	Molecular Function
NF-κB	Nuclear Factor kappa-light-chain-enhancer of Activated B cells
TS	Thymidylate Synthase
CSC	Cancer Stem Cell
15-LOX	15-Lipoxygenase

Supplementary Information

Table S1. Gut inflammation-related 755 targets retrieved from the GeneCard database, associated with CC retrieved from the GeneCards database.
Table S2. Gut inflammation-related unique 755 targets associated with CC were retrieved from the GeneCards database.
Table S3. USA-related 106 targets retrieved from the SwissTargetPrediction database.
Table S4. USA-related 86 targets retrieved from the SuperPred database.
Table S5. USA-related 181 unique targets retrieved from the SwissTargetPrediction and SuperPred database.
Table S6. 19 overlapping targets from Venny software using 755 targets associated with CC and 181 targets associated with USA.
Table S7. Protein-Protein Interaction (PPI) using 19 overlapping targets from the STRING database.
Table S8. Biological Process (BP) data of Gene Ontology (GO).
Table S9. Cellular Component (CC) data of Gene Ontology (GO).
Table S10. Molecular Function (MF) data of Gene Ontology (GO).
Table S11. KEGG signaling pathway.

Download link

References

1. Sung, H.; Ferlay, J.; Siegel, R.L.; Laversanne, M.; Soerjomataram, I.; Jemal, A.; Bray, F. Global Cancer Statistics 2020: GLOBOCAN Estimates of Incidence and Mortality Worldwide for 36 Cancers in 185 Countries. *CA Cancer J. Clin.* **2021**, *71*, 209-249, https://doi.org/10.3322/caac.21660.
2. Yang, B.; Wang, C.; Chen, X.; Zhai, H.; Wu, Y.; Cui, M.; Wu, J.; Li, W.; Hua, B. In silico and animal studies on the anti-cancer mechanisms of Shaoyao Decoction against colitis-associated colorectal cancer. *J. Ethnopharmacol.* **2025**, *345*, 119444, https://doi.org/10.1016/j.jep.2025.119444.
3. Qin, X.; Ge, L.; Wu, S.; Li, W. Association of dietary intake with cancer of the digestive system: a cross-sectional study. *Front. Nutr.* **2025**, *12*, 1539401, https://doi.org/10.3389/fnut.2025.1539401.
4. Fan, J.; Liu, Y.; Wang, J.; Yao, T.; Bai, S.; Ma, X.; Chen, H.; Chen, Y.; Gao, H.; Guo, Y.; Huang, H. NMB promotes the progression of colorectal cancer by regulating the NF-κB/P65 signaling pathway. *Front. Immunol.* **2025**, *16*, 1596451, https://doi.org/10.3389/fimmu.2025.1596451.
5. Itzkowitz, S.H.; Yio, X. Inflammation and Cancer IV. Colorectal cancer in inflammatory bowel disease: the role of inflammation. *Am. J. Physiol. - Gastrointest. Liver Physiol.* **2004**, *287*, G7-G17, https://doi.org/10.1152/ajpgi.00079.2004.
6. Ma, M.; Zheng, Z.; Li, J.; He, Y.; Kang, W.; Ye, X. Association between the gut microbiota, inflammatory factors, and colorectal cancer: evidence from Mendelian randomization analysis. *Front. Microbiol.* **2024**, *15*, 1309111, https://doi.org/10.3389/fmicb.2024.1309111.
7. Rizzo, A.; Pallone, F.; Monteleone, G.; Fantini, M.C. Intestinal inflammation and colorectal cancer: A double-edged sword?. *World J. Gastroenterol.* **2011**, *17*, 3092–3100.
8. Sánchez-Alcoholado, L.; Ramos-Molina, B.; Otero, A.; Laborda-Illanes, A.; Ordóñez, R.; Medina, J.A.; Gómez-Millán, J.; Queipo-Ortuño, M.I. The Role of the Gut Microbiome in Colorectal Cancer Development and Therapy Response. *Cancers* **2020**, *12*, 1406, https://doi.org/10.3390/cancers12061406.
9. Kim, J.; Lee, H.K. Potential Role of the Gut Microbiome In Colorectal Cancer Progression. *Front. Immunol.* **2022**, *12*, 807648, https://doi.org/10.3389/fimmu.2021.807648.
10. Wang, D.; DuBois, R.N. Pro-inflammatory prostaglandins and progression of colorectal cancer. *Cancer Lett.* **2008**, *267*, 197–203, https://doi.org/10.1016/j.canlet.2008.03.004.
11. Pannunzio, A.; Coluccia, M. Cyclooxygenase-1 (COX-1) and COX-1 Inhibitors in Cancer: A Review of Oncology and Medicinal Chemistry Literature. *Pharmaceuticals* **2018**, *11*, 101, https://doi.org/10.3390/ph11040101.
12. Jensen, T.S.R.; Mahmood, B.; Damm, M.B.; Backe, M.B.; Dahllöf, M.S.; Poulsen, S.S.; Hansen, M.B.; Bindslev, N. Combined activity of COX-1 and COX-2 is increased in non-neoplastic colonic mucosa from colorectal neoplasia patients. *BMC Gastroenterol.* **2018**, *18*, 31, https://doi.org/10.1186/s12876-018-0759-1.
13. Newman, P.; Muscat, J. Potential Role of Non-Steroidal Anti-Inflammatory Drugs in Colorectal Cancer Chemoprevention for Inflammatory Bowel Disease: An Umbrella Review. *Cancers* **2023**, *15*, 1102, https://doi.org/10.3390/cancers15041102.
14. Ganduri, V.; Rajasekaran, K.; Duraiyarasan, S.; Adefuye, M.A.; Manjunatha, N. Colorectal carcinoma, cyclooxygenases, and Cox inhibitors. *Cureus* **2022**, *14*, e28579, https://doi.org/10.7759/cureus.28579.
15. Atanasov, A.G.; Zotchev, S.B.; Dirsch, V.M.; Orhan, I.E.; Banach, M.; Rollinger, J.M.; Barreca, D.; Weckwerth, W.; Bauer, R.; Bayer, E.A.; Majeed, M.; Bishayee, A.; Bochkov, V.; Bonn, G.K.; Braidy, N.; Bucar, F.; Cifuentes, A.; D'Onofrio, G.; Bodkin, M.; Diederich, M.; Dinkova-Kostova, A.T.; Efferth, T.; El Bairi, K.; Arkells, N.; Fan, T.-P.; Fiebich, B.L.; Freissmuth, M.; Georgiev, M.I.; Gibbons, S.; Godfrey, K.M.; Gruber, C.W.; Heer, J.; Huber, L.A.; Ibanez, E.; Kijjoa, A.; Kiss, A.K.; Lu, A.; Macias, F.A.; Miller, M.J.S.; Mocan, A.; Müller, R.; Nicoletti, F.; Perry, G.; Pittalà, V.; Rastrelli, L.; Ristow, M.; Russo, G.L.; Silva, A.S.; Schuster, D.; Sheridan, H.; Skalicka-Woźniak, K.; Skaltsounis, L.; Sobarzo-Sánchez, E.; Bredt, D.S.; Stuppner, H.; Sureda, A.; Tzvetkov, N.T.; Vacca, R.A.; Aggarwal, B.B.; Battino, M.; Giampieri, F.; Wink, M.; Wolfender, J.-L.; Xiao, J.; Yeung, A.W.K.; Lizard, G.; Popp, M.A.; Heinrich, M.; Berindan-Neagoe, I.; Stadler, M.; Daglia, M.; Verpoorte, R.; Supuran, C.T.; the International Natural Product Sciences, T. Natural products in drug discovery: advances and opportunities. *Nature Reviews Drug Discovery* **2021**, *20*, 200-216, https://doi.org/10.1038/s41573-020-00114-z.
16. Domingo-Fernández, D.; Gadiya, Y.; Preto, A.J.; Krettler, C.A.; Mubeen, S.; Allen, A.; Healey, D.; Colluru, V. Natural Products Have Increased Rates of Clinical Trial Success throughout the Drug Development Process. *J. Nat. Prod.* **2024**, *87*, 1844-1851, https://doi.org/10.1021/acs.jnatprod.4c00581.

17. Ślusarczyk, J.; Adamska, E.; Czerwik-Marcinkowska, J. Fungi and Algae as Sources of Medicinal and Other Biologically Active Compounds: A Review. *Nutrients* **2021**, *13*, 3178, https://doi.org/10.3390/nu13093178.
18. Poulsen-Silva, E.; Gordillo-Fuenzalida, F.; Atala, C.; Moreno, A.A.; Otero, M.C. Bioactive Lichen Secondary Metabolites and Their Presence in Species from Chile. *Metabolites* **2023**, *13*, 805, https://doi.org/10.3390/metabo13070805.
19. Omarsdottir, S.; Olafsdottir, E.S.; Freysdottir, J. Immunomodulating effects of lichen-derived polysaccharides on monocyte-derived dendritic cells. *Int. Immunopharmacol.* **2006**, *6*, 1642–1650, https://doi.org/10.1016/j.intimp.2006.06.006.
20. Shahid, M.; Rasool, A.; Anjum, F.; Rehman, M.T. Biomedical Perspectives of Lichen-Derived Products. In Lichen-Derived Products; Yusuf, M., Ed.; Wiley: **2020**; pp. 263-276, https://doi.org/10.1002/9781119593249.ch12.
21. Esimone, C.O.; Grunwald, T.; Nworu, C.S.; Kuate, S.; Proksch, P.; Überla, K. Broad Spectrum Antiviral Fractions from the Lichen *Ramalina farinacea* (L.) Ach. *Chemotherapy* **2009**, *55*, 119-126, https://doi.org/10.1159/000194974.
22. Müller, K. Pharmaceutically relevant metabolites from lichens. *Appl. Microbiol. Biotechnol.* **2001**, *56*, 9–16, https://doi.org/10.1007/s002530100684.
23. Ahmed, M.Z.; Rao, T.; Khan, N.A.; Aslam, M.; Pane, Y.S. Antimicrobial Activities of Lichens. In Chemistry, Biology and Pharmacology of Lichen; Das, A.K., Sharma, A., Kathuria, D., Ansari, M.J., Bhardwaj, G., Eds.; Wiley: **2024**; pp. 169-191, https://doi.org/10.1002/9781394190706.ch13.
24. Ren, M.; Jiang, S.; Wang, Y.; Pan, X.; Pan, F.; Wei, X. Discovery and excavation of lichen bioactive natural products. *Front. Microbiol.* **2023**, *14*, 1177123, https://doi.org/10.3389/fmicb.2023.1177123.
25. Ingólfsdóttir, K. Usnic acid. *Phytochemistry* **2002**, *61*, 729–736, https://doi.org/10.1016/S0031-9422(02)00383-7.
26. Musatat, A.B.; Sevinç, Ö.S. Computational exploration of lichen secondary metabolite usnic acid: electronic properties, ADMET profiling, and antiviral potential against dengue virus NS5 protein. *Struct. Chem.* **2025**, https://doi.org/10.1007/s11224-025-02562-y.
27. Sujatha, D.; Hepsiba Rani, C.; Begum, S.; Sampathi, S.; Shah, S. In Silico, In Vitro and In Vivo Anti-inflammatory and Analgesic Activity of Usnic Acid. In Advances in Computational and Bio-Engineering; Jyothi, S., Mamatha, D., Satapathy, S., Raju, K., Favorskaya, M., Eds.; Springer: Cham, **2020**; Volume 15, pp. 249-261, https://doi.org/10.1007/978-3-030-46939-9_22.
28. Wenbing, W.; Hui, G.; Jingying, D.; Xiaolong, Y.; Yanan, Z.; Heng, P.; Dan, C.; Ruiman, G.; Lihong, C.; Ji, L. Usnic Acid Inhibits Proliferation and Migration through ATM Mediated DNA Damage Response in RKO Colorectal Cancer Cell. *Curr. Pharm. Biotechnol.* **2021**, *22*, 1129-1138, https://doi.org/10.2174/1389201021666201002155955.
29. Paudel, B.; Bhattarai, H.D.; Lee, H.K.; Oh, H.; Shin, H.W.; Yim, J.H. Antibacterial Activities of Ramalin, Usnic Acid and its Three Derivatives Isolated from the Antarctic Lichen Ramalina terebrata. *Z. Naturforsch. C.* **2010**, *65*, 34-38, https://doi.org/10.1515/znc-2010-1-206.
30. Agu, P.C.; Afiukwa, C.A.; Orji, O.U.; Ezeh, E.M.; Ofoke, I.H.; Ogbu, C.O.; Ugwuja, E.I.; Aja, P.M. Molecular docking as a tool for the discovery of molecular targets of nutraceuticals in diseases management. *Sci. Rep.* **2023**, *13*, 13398, https://doi.org/10.1038/s41598-023-40160-2.
31. Salo-Ahen, O.M.H.; Alanko, I.; Bhadane, R.; Bonvin, A.M.J.J.; Honorato, R.V.; Hossain, S.; Juffer, A.H.; Kabedev, A.; Lahtela-Kakkonen, M.; Larsen, A.S.; Lescrinier, E.; Marimuthu, P.; Mirza, M.U.; Mustafa, G.; Nunes-Alves, A.; Pantsar, T.; Saadabadi, A.; Singaravelu, K.; Vanmeert, M. Molecular Dynamics Simulations in Drug Discovery and Pharmaceutical Development. *Processes* **2021**, *9*, 71, https://doi.org/10.3390/pr9010071.
32. Subhaswaraj, P.; Siddhardha, B. Chapter 11 - Molecular docking and molecular dynamic simulation approaches for drug development and repurposing of drugs for severe acute respiratory syndrome-Coronavirus-2. In Computational Approaches for Novel Therapeutic and Diagnostic Designing to Mitigate SARS-CoV-2 Infection, Parihar, A., Khan, R., Kumar, A., Kaushik, A.K., Gohel, H., Eds.; Academic Press: **2022**; pp. 207-246, https://doi.org/10.1016/B978-0-323-91172-6.00007-8.
33. Ugbaja, S.C.; Mushebenge, A.G.-A.; Kumalo, H.; Ngcobo, M.; Gqaleni, N. Potential Benefits of In Silico Methods: A Promising Alternative in Natural Compound's Drug Discovery and Repurposing for HBV Therapy. *Pharmaceuticals* **2025**, *18*, 419, https://doi.org/10.3390/ph18030419.

34. Vikhar Danish Ahmad, A.; Khan, S.W.; Ali, S.A.; Yasar, Q. Network pharmacology combined with molecular docking and experimental verification to elucidate the effect of flavan-3-ols and aromatic resin on anxiety. *Sci. Rep.* **2024**, *14*, 9799, https://doi.org/10.1038/s41598-024-58877-z.
35. Ahmad, A.V.D.; Ali, S.A.; Yasar, Q.; Sakle, N.S.; Khan, M.M. Integrative network pharmacology, molecular docking, and dynamic simulation analysis of a polyherbal formulation for potential therapeutic impact on prostate cancer. *Heliyon* **2024**, *10*, e34531, https://doi.org/10.1016/j.heliyon.2024.e34531.
36. Roney, M.; Mohd Aluwi, M.F.F. The importance of in-silico studies in drug discovery. *Intell. Pharm.* **2024**, *2*, 578–579, https://doi.org/10.1016/j.ipha.2024.01.010.
37. Olajide, M.; Abdul-Hammed, M.; Bello, I.A.; Adedotun, I.O.; Afolabi, T.I. Identification of potential inhibitors of thymidylate synthase (TS) (PDB ID: 6QXH) and nuclear factor kappa-B (NF–κB) (PDB ID: 1A3Q) from *Capsicum annuum* (bell pepper) towards the development of new therapeutic drugs against colorectal cancer (CRC). *Phys. Sci. Rev.* **2024**, *9*, 1765-1798, https://doi.org/10.1515/psr-2022-0281.
38. Sidhu, R.S.; Lee, J.Y.; Yuan, C.; Smith, W.L. Comparison of Cyclooxygenase-1 Crystal Structures: Cross-Talk between Monomers Comprising Cyclooxygenase-1 Homodimers. *Biochemistry* **2010**, *49*, 7069-7079, https://doi.org/10.1021/bi1003298.
39. Hamim, S.M.I.; Roney, M.; Uddin, M.N.; Issahaku, A.R.; Chhando, K.S.; Aluwi, M.F.F.M.; Omar, N.A.M. Investigating the potential compounds of *Kalanchoe pinnata* plant for the treatment of inflammation utilizing molecular docking and molecular dynamic simulation approach. *In Silico Res. Biomed.* **2025**, *1*, 100007, https://doi.org/10.1016/j.insi.2025.100007.
40. Mun, C.S.; Hui, L.Y.; Sing, L.C.; Karunakaran, R.; Ravichandran, V. Multi-targeted molecular docking, pharmacokinetics, and drug-likeness evaluation of coumarin based compounds targeting proteins involved in development of COVID-19. *Saudi J. Biol. Sci.* **2022**, *29*, 103458, https://doi.org/10.1016/j.sjbs.2022.103458.
41. Ahsin, A.; Kurbanova, M.; Ahmad, S.; Qamar, A.; Ashfaq, M.; Tahir, M.N.; Dege, N.; Şahin, O.; Abuelizz, H.A.; Al-Salahi, R.; El Bakri, Y. Synthesis, structure, supramolecular assembly inspection by Hirshfeld surface analysis, DFT study and molecular docking inspection of 4,5-bis(2-chlorophenyl)-8a-phenylhexahydropyrimido[4,5-d]pyrimidine-2,7(1*H*,3*H*)-dithione. *J. Mol. Struct.* **2025**, *1319*, 139580, https://doi.org/10.1016/j.molstruc.2024.139580.
42. Roney, M.; Uddin, M.N.; Khan, A.A.; Fatima, S.; Mohd Aluwi, M.F.F.; Hamim, S.M.I.; Ahmad, A. Repurposing of dipeptidyl peptidase FDA-approved drugs in Alzheimer's disease using network pharmacology and in-silico approaches. *Comput. Biol. Chem.* **2025**, *116*, 108378, https://doi.org/10.1016/j.compbiolchem.2025.108378.
43. Pant, J.; Mittal, P.; Singh, L.; Marwah, H. Canthaxanthin downregulates EGFR in NSCLC: network pharmacology, molecular docking, dynamics simulations, ADMET, and in-vitro analysis. *Mol. Divers.* **2026**, *30*, 1071-1092, https://doi.org/10.1007/s11030-025-11246-y.
44. Roney, M.; Issahaku, A.R.; Khan, A.A.; Fatima, S.; Hamim, S.M.I.; Mohd Aluwi, M.F.F.; Wilhelm, A.; Ahmad, A. In Silico Evaluation of Approved Drug Library to Discover Tyrosine Threonine Kinase Inhibitors for Colon Cancer. *ChemistrySelect* **2025**, *10*, e202500093, https://doi.org/10.1002/slct.202500093.
45. Roney, M.; Issahaku, A.R.; Hamim, S.M.I.; Wilhelm, A.; Mohd Aluwi, M.F.F. Repurposing Sulfonamide-Based Antidiabetic Agents Against Polycystic Ovary Syndrome: A Molecular Docking and Dynamics Simulation Approach. *is J. Pharm. Innov.* **2025**, *20*, 202, https://doi.org/10.1007/s12247-025-10119-z.
46. Hou, H.; Liu, X.; Liu, W.; Zhang, P.; Zhou, B. Warhead-bearing natural compounds for multi-pathway irreversible inhibition to overcome drug resistance in colorectal cancer. *Med. Oncol.* **2025**, *42*, 148, https://doi.org/10.1007/s12032-025-02699-0.
47. Santos, T.M.R.; Tavares, C.A.; Pereira, A.F.; da Cunha, E.F.F.; Ramalho, T.C. Evaluation of autophagy inhibition to combat cancer: (vanadium complex)–protein interactions, parameterization, and validation of a new force field. *J. Mol. Model.* **2023**, *29*, 123, https://doi.org/10.1007/s00894-023-05530-7.
48. Issahaku, A.R.; Soliman, M. Camptothecin and its Analogues as Putative Bruton Tyrosine Kinase (BTK) Inhibitors in Cancer Therapy - Biophysical Simulations of Wild Type and C481S Mutation. *J. Cancer Biomol. Ther.* **2024**, *1*, 59-71, https://doi.org/10.62382/jcbt.v1i1.10.
49. Li, L.; Mohammed, A.H.; Auda, N.A.; Alsallameh, S.M.S.; Albekairi, N.A.; Muhseen, Z.T.; Butch, C.J. Network Pharmacology, Molecular Docking, and Molecular Dynamics Simulation Analysis Reveal Insights into the Molecular Mechanism of *Cordia myxa* in the Treatment of Liver Cancer. *Biology* **2024**, *13*, 315, https://doi.org/10.3390/biology13050315.

50. Ngernsombat, C.; Suriya, U.; Prattapong, P.; Verma, K.; Rungrotmongkol, T.; Soonkum, T.; Kuhaudomlarp, S.; Janvilisri, T. Repurposing FDA-approved drugs targeting FZD10 in nasopharyngeal carcinoma: insights from molecular dynamics simulations and experimental validation. *Sci. Rep.* **2024**, *14*, 31461, https://doi.org/10.1038/s41598-024-82967-7.
51. Aisha, I.E.h.; Ahmed El, R.; Mahmoud, E.S.S. Comparative Dynamic Features of Apo and Bound MDM2 Protein Reveal the Mechanism of Inhibitor Recognition for Anti-Cancer Activity. *Curr. Med. Chem.* **2023**, *30*, 1193-1206, https://doi.org/10.2174/0929867329666220610194919.
52. Roney, M.; Issahaku, A.R.; Dubey, A.; Tufail, A.; Istiaque Hamim, S.M.; Wilhelm, A.; Aluwi, M.F.F.M. In-silico evaluation of diffractaic acid as novel anti-diabetic inhibitor against dipeptidyl peptidase IV enzyme. *In Silico Pharmacol.* **2025**, *13*, 24, https://doi.org/10.1007/s40203-025-00321-9.
53. Roney, M.; Issahaku, A.R.; Govinden, U.; Gazali, A.M.; Aluwi, M.F.F.M.; Zamri, N.B. Diabetic wound healing of aloe vera major phytoconstituents through TGF-β1 suppression *via in-silico* docking, molecular dynamic simulation and pharmacokinetic studies. *J. Biomol. Struct. Dyn.* **2024**, *42*, 13939-13952, https://doi.org/10.1080/07391102.2023.2279280.
54. Li, X.; Lin, B.; Lin, Z.; Ma, Y.; Wang, Q.; Zheng, Y.; Cui, L.; Luo, H.; Luo, L. Exploration in the mechanism of fucosterol for the treatment of non-small cell lung cancer based on network pharmacology and molecular docking. *Sci. Rep.* **2021**, *11*, 4901, https://doi.org/10.1038/s41598-021-84380-w.
55. Wang, S.; Chen, W.; Dong, C.; Wu, J.; Zheng, M.; Ma, Y.; Xue, Y. Exploring the mechanism of genistein in treating hepatocellular carcinoma through network pharmacology and molecular docking. *Oncologie* **2024**, *26*, 799–811, https://doi.org/10.1515/oncologie-2024-0304.
56. Dong, H.; Li, M.; Chen, H.; Tian, L.; Wei, W.; Wang, S.; Cheng, G.; Liu, S. Using network pharmacological analysis and molecular docking to investigate the mechanism of action of quercetin's suppression of oral cancer. *J. Cancer Res. Clin. Oncol.* **2023**, *149*, 15055-15067, https://doi.org/10.1007/s00432-023-05290-0.
57. He, R.; Ou, S.; Chen, S.; Ding, S. Network Pharmacology-Based Study on the Molecular Biological Mechanism of Action for Compound Kushen Injection in Anti-Cancer Effect. *Med. Sci. Monit.* **2020**, *26*, e918520, https://doi.org/10.12659/MSM.918520.
58. Lalmuansangi, C.; Lalfakawmi; Nghakliana, F.; Sailo, H.; Tochhawng, L.; Trivedi, A.K.; Kharat, K.R.; Vellingiri, B.; Kumar, N.S.; Siama, Z. Anticancer activity of Stemona tuberosa (wild asparagus) against type-II human lung adenocarcinoma (A549) cells and identification of SRC inhibitor using integrated network pharmacology and molecular dynamic simulation. *Discov. Oncol.* **2025**, *16*, 429, https://doi.org/10.1007/s12672-025-02138-6.
59. Xi, P.; Niu, Y.; Zhang, Y.; Li, W.; Gao, F.; Gu, W.; Kui, F.; Liu, Z.; Lu, L.; Du, G. The mechanism of dioscin preventing lung cancer based on network pharmacology and experimental validation. *J. Ethnopharmacol.* **2022**, *292*, 115138, https://doi.org/10.1016/j.jep.2022.115138.
60. Chen, G.; Seukep, A.J.; Guo, M. Recent Advances in Molecular Docking for the Research and Discovery of Potential Marine Drugs. *Mar. Drugs* **2020**, *18*, 545, https://doi.org/10.3390/md18110545.
61. Mfotie Njoya, E.; Ndemangou, B.; Akinyelu, J.; Munvera, A.M.; Chukwuma, C.I.; Mkounga, P.; Mashele, S.S.; Makhafola, T.J.; McGaw, L.J. *In vitro* antiproliferative, anti-inflammatory effects and molecular docking studies of natural compounds isolated from *Sarcocephalus pobeguinii* (Hua ex Pobég). *Front. Pharmacol.* **2023**, *14*, 1205414, https://doi.org/10.3389/fphar.2023.1205414.
62. Bharathi, R.; Santhi, N. In vitro and molecular docking studies of an antiinflammatory scaffold with human peroxiredoxin 5 and tyrosine kinase receptor. *Bioinformation* **2020**, *16*, 929–936, https://doi.org/10.6026/97320630016929.
63. Sahoo, R.N.; Pattanaik, S.; Pattnaik, G.; Mallick, S.; Mohapatra, R. Review on the use of Molecular Docking as the First Line Tool in Drug Discovery and Development. *Indian J. Pharm. Sci.* **2022**, *84*, 1334–1337, https://doi.org/10.36468/pharmaceutical-sciences.1031.
64. Ahmad, V.; Khan, M.I.; Jamal, Q.M.S.; Alzahrani, F.A.; Albiheyri, R. Computational Molecular Docking and Simulation-Based Assessment of Anti-Inflammatory Properties of *Nyctanthes arbor-tristis Linn* Phytochemicals. *Pharmaceuticals* **2024**, *17*, 18, https://doi.org/10.3390/ph17010018.
65. Vodenkova, S.; Buchler, T.; Cervena, K.; Veskrnova, V.; Vodicka, P.; Vymetalkova, V. 5-fluorouracil and other fluoropyrimidines in colorectal cancer: Past, present and future. *Pharmacol. Ther.* **2020**, *206*, 107447, https://doi.org/10.1016/j.pharmthera.2019.107447.

66. Alzahrani, S.M.; Al Doghaither, H.A.; Al-ghafari, A.B.; Pushparaj, P.N. 5-Fluorouracil and capecitabine therapies for the treatment of colorectal cancer (Review). *Oncol. Rep.* **2023**, *50*, 175, https://doi.org/10.3892/or.2023.8612.
67. Cho, Y.-H.; Ro, E.J.; Yoon, J.-S.; Mizutani, T.; Kang, D.-W.; Park, J.-C.; Il Kim, T.; Clevers, H.; Choi, K.-Y. 5-FU promotes stemness of colorectal cancer via p53-mediated WNT/β-catenin pathway activation. *Nat. Commun.* **2020**, *11*, 5321, https://doi.org/10.1038/s41467-020-19173-2.
68. Sommer, J.; Mahli, A.; Freese, K.; Schiergens, T.S.; Kuecuekoktay, F.S.; Teufel, A.; Thasler, W.E.; Müller, M.; Bosserhoff, A.K.; Hellerbrand, C. Analysis of molecular mechanisms of 5-fluorouracil-induced steatosis and inflammation in vitro and in mice. *Oncotarget* **2016**, *8*, 13059–13072, https://doi.org/10.18632/oncotarget.14371.
69. Alhoshani, N.M.; Al-Zharani, M.; Almutairi, B.; Aljarba, N.H.; Al-Johani, N.S.; Alkeraishan, N.; AlKahtane, A.A.; Alarifi, S.; Ali, D.; Alkahtani, S. Antioxidant and anti-inflammatory activities of lycopene against 5-fluorouracil-induced cytotoxicity in Caco2 cells. *Saudi Pharm. J.* **2022**, *30*, 1665-1671, https://doi.org/10.1016/j.jsps.2022.09.011.
70. He, S.; Wang, Z.; Xia, J.; Jia, H.; Dai, Q.; Chen, C.; He, F.; Wang, X.; Zhou, M. Dasabuvir alleviates 5-fluorouracil-induced intestinal injury through anti-senescence and anti-inflammatory. *Sci. Rep.* **2024**, *14*, 15730, https://doi.org/10.1038/s41598-024-66771-x.
71. Bai, S.-r.; Zhao, B.-x.; Zhao, Q.; Ge, Y.-c.; Li, M.; Zhao, C.-g.; Wu, X.-j.; Wang, X.-b. Oleanolic acid improves 5-fluorouracil-induced intestinal damage and inflammation by alleviating intestinal senescence. *Sci. Rep.* **2024**, *14*, 21852, https://doi.org/10.1038/s41598-024-72536-3.
72. Tsujii, M.; Kawano, S.; Tsuji, S.; Sawaoko, H.; Hori, M.; DuBois, R.N. Cyclooxygenase Regulates Angiogenesis Induced by Colon Cancer Cells. *Cell* **1998**, *94*, P273, https://doi.org/10.1016/S0092-8674(02)09420-5.
73. Sano, H.; Kawahito, Y.; Wilder, R.L.; Hashiramoto, A.; Mukai, S.; Asai, K.; Kimura, S.; Kato, H.; Kondo, M.; Hla, T. Expression of CyclooxygenÃ¤se-1and -2 in Human Colorectal Cancer. *Cancer Res.* **1995**, *55*, 3785-3789.
74. Morris, G.M.; Huey, R.; Lindstrom, W.; Sanner, M.F.; Belew, R.K.; Goodsell, D.S.; Olson, A.J. AutoDock4 and AutoDockTools4: Automated docking with selective receptor flexibility. *J. Comput. Chem.* **2009**, *30*, 2785-2791,https://doi.org/10.1002/jcc.21256.
75. Xuan-Yu, M.; Hong-Xing, Z.; Mihaly, M.; Meng, C. Molecular Docking: A Powerful Approach for Structure-Based Drug Discovery. *Curr. Comput. Aided Drug Des.* **2011**, *7*, 146-157, https://doi.org/10.2174/157340911795677602.
76. Oladoja, F.A.; Awodele, O.; Oreagba, I.A.; Irokosu, E.S.; Oyinloye, E.O.; Murtala, A.A. Anti-inflammatory activity and molecular docking studies of the hydromethanolic leaf extract of *Baphia longipedicellata* brumitt in rats. *Pharmacol. Res. Mod. Chin. Med.* **2024**, *13*, 100512, https://doi.org/10.1016/j.prmcm.2024.100512.
77. Canyelles-Niño, M.; González-Lafont, À.; Lluch, J.M. Hydroperoxidation of Docosahexaenoic Acid by Human ALOX12 and pigALOX15-mini-LOX. *Int. J. Mol. Sci.* **2023**, *24*, 6064, https://doi.org/10.3390/ijms24076064.
78. Paździora, W.; Podolak, I.; Grudzińska, M.; Paśko, P.; Grabowska, K.; Galanty, A. Critical Assessment of the Anti-Inflammatory Potential of Usnic Acid and Its Derivatives—A Review. *Life* **2023**, *13*, 1046, https://doi.org/10.3390/life13041046.
79. Kwon, Y.; Magnuson, B.A. Effect of azoxymethane and curcumin on transcriptional levels of cyclooxygenase-1 and -2 during initiation of colon carcinogenesis. *Scand. J. Gastroenterol.* **2007**, *42*, 72-80, https://doi.org/10.1080/00365520600825216.
80. Crescente, M.; Jessen, G.; Momi, S.; Höltje, H.-D.; Gresele, P.; Cerletti, C.; de Gaetano, G. Interactions of gallic acid, resveratrol, quercetin and aspirin at the platelet cyclooxygenase-1 level Functional and modelling studies. *Thromb. Haemost.* **2009**, *102*, 336-346, https://doi.org/10.1160/TH09-01-0057.
81. Kang, S.S.; Cuendet, M.; Endringer, D.C.; Croy, V.L.; Pezzuto, J.M.; Lipton, M.A. Synthesis and biological evaluation of a library of resveratrol analogues as inhibitors of COX-1, COX-2 and NF-κB. *Bioorg. Med. Chem.* **2009**, *17*, 1044-1054, https://doi.org/10.1016/j.bmc.2008.04.031.
82. Liang, Y.-C.; Huang, Y.-T.; Tsai, S.-H.; Lin-Shiau, S.-Y.; Chen, C.-F.; Lin, J.-K. Suppression of inducible cyclooxygenase and inducible nitric oxide synthase by apigenin and related flavonoids in mouse macrophages. *Carcinogenesis* **1999**, *20*, 1945-1952, https://doi.org/10.1093/carcin/20.10.1945.

83. Seeram, N.P.; Zhang, Y.; Nair, M.G. Inhibition of Proliferation of Human Cancer Cells and Cyclooxygenase Enzymes by Anthocyanidins and Catechins. *Nutr. Cancer* **2003**, *46*, 101–106, https://doi.org/10.1207/S15327914NC4601_13.
84. Barua, J.; Sany, M.A.; Barua, L.; Hossen, M.; Absar, N.; Hossain, Z.; Begum, H.; Akther, S.; Akther, N.A.S.; Akther, S. Insilico molecular docking of some isolated selected compounds of Phoenix Sylvestris (L.) against diabetes. *Biomed. J. Sci. Tech. Res.* **2019**, *16*, 1-4, https://doi.org/10.26717/BJSTR.2019.16.002819.
85. Nunthanavanit, P.; Samee, W. Molecular Docking of Natural Product-Derived Compounds: Estimation of Selectivity on Cyclo-oxygenase-2. *Thai Pharm. Health Sci. J.* **2011**, *6*, 79–85.
86. Ghahremanian, S.; Rashidi, M.M.; Raeisi, K.; Toghraie, D. Molecular dynamics simulation approach for discovering potential inhibitors against SARS-CoV-2: A structural review. *J. Mol. Liq.* **2022**, *354*, 118901, https://doi.org/10.1016/j.molliq.2022.118901.
87. Adelusi, T.I.; Oyedele, A.-Q.K.; Boyenle, I.D.; Ogunlana, A.T.; Adeyemi, R.O.; Ukachi, C.D.; Idris, M.O.; Olaoba, O.T.; Adedotun, I.O.; Kolawole, O.E.; Xiaoxing, Y.; Abdul-Hammed, M. Molecular modeling in drug discovery. *Inform. Med. Unlocked* **2022**, *29*, 100880, https://doi.org/10.1016/j.imu.2022.100880.
88. Hollingsworth, S.A.; Dror, R.O. Molecular Dynamics Simulation for All. *Neuron* **2018**, *99*, 1129–1143, https://doi.org/10.1016/j.neuron.2018.08.011.
89. Koonammackal, M.V.; Nellipparambil, U.V.N.; Sudarsanakumar, C. Molecular dynamics simulations and binding free energy analysis of DNA minor groove complexes of curcumin. *J. Mol. Model.* **2011**, *17*, 2805-2816, https://doi.org/10.1007/s00894-011-0954-2.
90. Fatriansyah, J.F.; Rizqillah, R.K.; Yandi, M.Y.; Sahlan, M. Molecular docking and dynamics studies on propolis sulabiroin-A as a potential inhibitor of SARS-CoV-2. *J. King Saud Univ. - Sci.* **2022**, *34*, 101707, https://doi.org/10.1016/j.jksus.2021.101707.
91. Rampogu, S.; Lee, G.; Park, J.S.; Lee, K.W.; Kim, M.O. Molecular Docking and Molecular Dynamics Simulations Discover Curcumin Analogue as a Plausible Dual Inhibitor for SARS-CoV-2. *Int. J. Mol. Sci.* **2022**, *23*, 1771, https://doi.org/10.3390/ijms23031771.
92. Justino, G.C.; Nascimento, C.P.; Justino, M.C. Molecular dynamics simulations and analysis for bioinformatics undergraduate students. *Biochem. Mol. Biol. Educ.* **2021**, *49*, 570–582, https://doi.org/10.1002/bmb.21512.
93. Martins, J.M.; Ramos, R.M.; Pimenta, A.C.; Moreira, I.S. Solvent-accessible surface area: How well can be applied to hot-spot detection? *Proteins: Struct. Funct. Bioinform.* **2014**, *82*, 479–490, https://doi.org/10.1002/prot.24413.
94. Borjian Boroujeni, M.; Shahbazi Dastjerdeh, M.; Shokrgozar, M.; Rahimi, H.; Omidinia, E. Computational driven molecular dynamics simulation of keratinocyte growth factor behavior at different pH conditions. *Inform. Med. Unlocked* **2021**, *23*, 100514, https://doi.org/10.1016/j.imu.2021.100514.
95. Islam, R.; Parves, M.R.; Paul, A.S.; Uddin, N.; Rahman, M.S.; Mamun, A.A.; Hossain, M.N.; Ali, M.A.; Halim, M.A. A molecular modeling approach to identify effective antiviral phytochemicals against the main protease of SARS-CoV-2. *J. Biomol. Struct. Dyn.* **2021**, *39*, 3213-3224, https://doi.org/10.1080/07391102.2020.1761883.
96. Giuliani, A. The application of principal component analysis to drug discovery and biomedical data. *Drug Discov. Today* **2017**, *22*, 1069–1076, https://doi.org/10.1016/j.drudis.2017.01.005.
97. Hayat, C.; Subramaniyan, V.; Alamri, M.A.; Wong, L.S.; Khalid, A.; Abdalla, A.N.; Afridi, S.G.; Kumarasamy, V.; Wadood, A. Identification of new potent NLRP3 inhibitors by multi-level in-silico approaches. *BMC Chem.* **2024**, *18*, 76, https://doi.org/10.1186/s13065-024-01178-3.
98. dos Santos Nascimento, I.J.; De Souza, M.; Medeiros, D.C.; de Moura, R.O. Dynamic Cross-Correlation Matrix (DCCM) Reveals New Insights to Discover New NLRP3 Inhibitors Useful as Anti-Inflammatory Drugs. *Med. Sci. Forum* **2022**, *14*, 84, https://doi.org/10.3390/ECMC2022-13306.
99. Genheden, S.; Ryde, U. The MM/PBSA and MM/GBSA methods to estimate ligand-binding affinities. *Expert Opin. Drug Discov.* **2015**, *10*, 449–461, https://doi.org/10.1517/17460441.2015.1032936.
100. Dong, L.; Qu, X.; Zhao, Y.; Wang, B. Prediction of Binding Free Energy of Protein–Ligand Complexes with a Hybrid Molecular Mechanics/Generalized Born Surface Area and Machine Learning Method. *ACS Omega* **2021**, *6*, 32938–32947, https://doi.org/10.1021/acsomega.1c04996.
101. Tang, Y.-Y.; Wang, D.-C.; Wang, Y.-Q.; Huang, A.-F.; Xu, W.-D. Emerging role of hypoxia-inducible factor-1α in inflammatory autoimmune diseases: A comprehensive review. *Front. Immunol.* **2023**, *13*, 1073971, https://doi.org/10.3389/fimmu.2022.1073971.

102. Palazon, A.; Goldrath, A.W.; Nizet, V.; Johnson, R.S. HIF Transcription Factors, Inflammation, and Immunity. *Immunity* **2014**, *41*, P518–P528, https://doi.org/10.1016/j.immuni.2014.09.008.
103. McGettrick, A.F.; O'Neill, L.A.J. The Role of HIF in Immunity and Inflammation. *Cell Metab.* **2020**, *32*, P524–P536, https://doi.org/10.1016/j.cmet.2020.08.002.
104. Balamurugan, K. HIF-1 at the crossroads of hypoxia, inflammation, and cancer. *Int. J. Cancer* **2016**, *138*, 1058–1066, https://doi.org/10.1002/ijc.29519.
105. Tuncer, S.; Banerjee, S. Eicosanoid pathway in colorectal cancer: Recent updates. *World J. Gastroenterol* **2015**, *21*, 11748–11766, https://doi.org/10.3748/wjg.v21.i41.11748.
106. Nasry, W.H.S.; Martin, C.K. Intersecting Mechanisms of Hypoxia and Prostaglandin E2-Mediated Inflammation in the Comparative Biology of Oral Squamous Cell Carcinoma. *Front. Oncol.* **2021**, *11*, 539361, https://doi.org/10.3389/fonc.2021.539361.
107. Li, Q.; Geng, S.; Luo, H.; Wang, W.; Mo, Y.-Q.; Luo, Q.; Wang, L.; Song, G.-B.; Sheng, J.-P.; Xu, B. Signaling pathways involved in colorectal cancer: pathogenesis and targeted therapy. *Signal Transduct. Target. Ther.* **2024**, *9*, 266, https://doi.org/10.1038/s41392-024-01953-7.
108. Liu, W.; Fan, X.; Jian, B.; Wen, D.; Wang, H.; Liu, Z.; Li, B. The signaling pathway of hypoxia inducible factor in regulating gut homeostasis. *Front. Microbiol.* **2023**, *14*, 1289102, https://doi.org/10.3389/fmicb.2023.1289102.
109. Aoki, T.; Narumiya, S. Prostaglandin E_2-EP2 signaling as a node of chronic inflammation in the colon tumor microenvironment. *Inflamm. Regen.* **2017**, *37*, 4, https://doi.org/10.1186/s41232-017-0036-7.
110. Chulada, P.C.; Thompson, M.B.; Mahler, J.F.; Doyle, C.M.; Gaul, B.W.; Lee, C.; Tiano, H.F.; Morham, S.G.; Smithies, O.; Langenbach, R. Genetic disruption of *Ptgs-1*, as well as *Ptgs-2*, reduces intestinal tumorigenesis in *Min* mice. *Cancer Res.* **2000**, *60*, 4705-4708.

Publisher's Note & Disclaimer